TESTING AND ENHANCED MODELLING OF PASSIVE EVOLUTIONARY SYSTEMS TECHNOLOGY FOR CONTAINMENT COOLING

TEMPEST

PROJECT CO-ORDINATOR

V.A. Wichers
NRG/PPT
Westerduinweg 3
NL-1755 Petten
THE NETHERLANDS
Tel.: +31 224 564 656
Fax: +31 224 563 490
E-mail: wichers@nrg-nl.com

SCIENTIFIC CO-ORDINATOR

M. Huggenberger
PSI/LTH
CH-5232 Villigen PSI
SWITZERLAND

Tel.: +41-56-310 4150
Fax: +41-56-310 4481
E-mail: max.huggenberger@psi.ch

PROJECT PARTNERS

1. NRG, Nuclear Research and Consultancy Group, Petten, The Netherlands
2. CEA, Commissariat à l`Energie Atomique, Cadarache, France
3. FZK, Forschungszentrum Karlsruhe, Karlsruhe, Germany
4. GRS, Gesellschaft für Anlagen und Reaktorsicherheit, Cologne, Germany
5. FANP, Framatome Advanced Nuclear Power, Offenbach, Germany
6. VTT, Technical Research Centre of Finland, Espoo, Finland
7. PSI, Paul Scherrer Institut, Villigen, Switzerland

CONTRACT N°: FIKS-CT-2000-00095

EC Contribution:	EUR 1.000.015
Total Project Value:	EUR 3.238.785
Starting Date:	December 2000
Duration:	36 Months

CONTENTS

LIST OF ABBREVIATIONS AND SYMBOLS

BC	Building Condenser
BDBA	Beyond Design Basis Accident
BWR	Boiling Water Reactor
CEA	Commissariat à l`Energie Atomique (France)
CFD	Computational Fluid Dynamics (code)
CFX	CFD code for fluid dynamics and heat transfer
COCOSYS	Containment analyses lumped parameter code
DBA	Design Basis Accident
DGRS	Drywell Gas Re-circulation System
DW	Drywell
ESBWR	European Simplified Boiling Water Reactor (General Electric)
FANP	Framatome Advanced Nuclear Power (Germany)
FLUENT	CFD code for fluid flow and heat transfer
FWP	Frame Work Programme
FZK	Forschungszentrum Karlsruhe (Germany)
GASFLOW	3D-fluid dynamics field code
GE	General Electric
GOTHIC	3D containment code
GRS	Gesellschaft für Anlagen- und Reaktorsicherheit
IPSS	Innovative Passive Safety Systems (4^{th} FWP Project)
KALI	Medium-scale thermal-hydraulic test facility at CEA, Cadarache
KWU	Kraftwerk Union
LOCA	Loss Of Coolant Accident
LP	Lumped Parameter (code)
LWR	Light Water Reactor
MELCOR	Severe accident lumped parameter code
MSLB	Main Steam Line Break
M-W	Metal-Water (reaction)
NACUSP	Natural Circulation and Stability Performance of BWRs (5^{th} FWP Project)
NPP	Nuclear Power Plant
NRG	Nuclear Research and Consultancy Group (The Netherlands)
PANDA	Large-scale multi-purpose thermal-hydraulic test facility at PSI, Switzerland
PCC	Passive Containment Cooler
PCCS	Passive Containment Cooling System
PSI	Paul Scherrer Institut (Switzerland)
RPV	Reactor Pressure Vessel
SBWR	Simplified Boiling Water Reactor (General Electric)
SOSV	Stuck Open Safety Valve
SPECTRA	Lumped parameter thermal-hydraulic code
SRV	Safety Relief Valve
STAR-CD	CFD code for fluidics and thermics
SWR1000	Siede Wasser Reaktor 1000 (Framatome-ANP)
TRACG	Transient Reactor Analysis Code (GE Version)
VTT	Valtion Teknillinen Tutkimuskeskus (Technical Research Centre of Finland)
WAVCO	Lumped parameter thermodynamic code
WW	Wetwell (Suppression Chamber)

EXECUTIVE SUMMARY

The main objective of TEMPEST was to validate and improve advanced modelling methods for evaluating pressure safety margins of BWR containments. Accurate prediction of pressure transients in case of accidents requires capabilities for modelling 3D effects such as mixing and stratification of steam, nitrogen and hydrogen in containment compartments. Computational Fluid Dynamics (CFD) codes and other advanced codes possess the desired capabilities. TEMPEST performed both experimental and analytical research in the areas of:

Validation of Building Condenser System Models.

The system behaviour of the SWR1000 containment with Building Condensers (BC) was investigated, by simulating the blow-down phase in case of a small leak in the upper part of the RPV and non-operation of the core flooding system. Knowledge of the distribution of non-condensable gases is essential because it may negatively affect the performance of the passive BC systems. Simulations were carried out with CFD codes and Lumped Parameter (LP) codes (CFX, STAR-CD, GASFLOW, COCOSYS, WAVCO, SPECTRA). From comparisons with existing PANDA data, it was concluded that only LP codes appear to be able to provide comprehensive predictions for complex long-time transients. Due to limitations in the models and available computer resources, CFD codes are either restricted to simulate selected periods or to include only parts of the problem. A recommendation could be, to use LP models to get an overview of a scenario and for parametric studies. CFD codes can be applied for specific, more detailed investigations. Combined LP/CFD approaches could be introduced to split the computational region or to improve the depth of modelling.

Passive Safety Features Assessment and Optimisation.

The performance of the Passive Containment Cooling System (PCCS) of the ESBWR was investigated in PANDA tests for accident scenarios including release of hydrogen from reactor core (H2 was simulated by He). During He-release the PCCS heat removal capability was degraded, but the considerable increase in containment pressure was mainly caused by the amount of gas released. Some time after He-release stopped and the gas was vented to the Wetwell (WW), the PCCS recovered and the pressure finally stabilized at higher level. A new accident mitigating system (DGRS) showed its capability to retain non-condensable gas in the Drywell (DW), thereby slightly reducing containment pressure. The gas stratification patterns observed in the DW could be well predicted by CFD codes (CFX, STAR-CD) and by the 3D code GOTHIC. CFX and FLUENT confirmed the complex flow pattern observed in PCCs during PANDA tests.

Wetwell Gas Space Modelling and Performance Assessment.

Tests performed in KALI provided an extended database concerning gas mixing and stratification. Hydrogen or helium and steam mixtures were injected into a closed vessel. The test conditions were close to the WW parameters used in the PANDA tests. In the KALI tests it was also investigated if He is suitable to substitute H2 in system tests, aimed to simulate containment and PCCS response in case of accidents with H2 release. KALI tests indicated that mixing/stratification behaviours are close for both gases. The stratification and mixing patterns calculated by CFX, STAR-CD and GOTHIC showed a qualitatively good agreement with the experimental data.

Plant Evaluation.

Improved models and insights based on the TEMPEST results have been translated to the plant level, in particular to SWR1000 and ESBWR. For the SWR1000, one severe accident scenario was analysed with SPECTRA and WAVCO. The system pressure stabilises when the

non-condensable gases are diluted to such a degree that the BC power matches steam release from the core. The discrepancy in containment pressure prediction is between 8-13%. Because LP codes are not suitable to predict detailed gas distributions, supplementary calculations with CFD codes are recommended to improve prediction quality.

A. OBJECTIVES AND SCOPE

The main objective of the TEMPEST project was to validate and improve advanced modelling methods for evaluating pressure safety margins of BWR containments [1]. Accurate prediction of containment pressure during accidents requires capabilities for modelling three-dimensional (3D) effects such as mixing and stratification, since these strongly affect the performance of passive cooling systems. Computational Fluid Dynamics (CFD) codes, but also other advanced modelling methods, possess the desired 3D capabilities. TEMPEST addressed both analytical and experimental research to support advances in different areas: The ability of CFD codes to predict passive safety system performance of SWR1000 [2] and ESBWR [3] has been validated for a broad range of accident conditions. Already existing experimental data and new data obtained in integral and separate-effect tests were used. Where necessary, the data have been used for model improvement purposes. New system tests have been carried out in PANDA to evaluate the effect of hydrogen on condenser performance. The effectiveness of the Drywell Gas Re-circulation System (DGRS) in lowering peak and long-term containment pressure has been investigated and the PCCS and DGRS systems interaction has also been tested. The ability of CFD codes to predict mixing and stratification in containments under severe accident conditions has been assessed. The required data were obtained from new experiments on mixing/stratification in hydrogen-steam-air atmospheres performed in separate-effect tests (KALI) and integral system tests (PANDA). Finally, the project results have been translated to the plant level.

B. WORK PROGRAMME

B.1Validation of Building Condenser System Models (WP1)

The motivation for this work was to validate various CFD codes and LP codes against existing data with respect to major phenomena occurring in passive cooling systems. The data from SWR1000 Building Condenser (BC) tests performed in the PANDA facility within the project IPSS (4^{th} FWP) have been evaluated. The tests were characterised with respect to significant phenomena (mixing/stratification, jets, plumes) and their major influences on the system response. The sensitivity of the BC and the test outcomes to boundary conditions were investigated by energy and mass balances based on measured data, backed up by energy balances based on results obtained with computer codes. The transportation and deposition of energy and distribution of species concentration between the facility components were quantified. Analysis of jet impingement in the DW vessel was carried-out with CFD calculations. CFD and LP models were validated against test results. Various CFD codes, LP codes and combinations of it were applied: Pool boiling on the secondary side of the BC has been analysed with CFX in order to assess the code capabilities to describe pool behaviour under two-phase conditions. GASFLOW and STAR-CD simulated containment phenomena in order to validate modelling of mixing, stratification and condensation. Full scope analysis, which features strong temperature stratification was performed with COCOSYS. WAVCO was applied for calculations that comprise BC primary side and secondary side, thus assessing the modelling of relevant phenomena. A coupled CFX/SPECTRA calculation was done for test BC4. The boundary conditions for the CFX calculation were provided by SPECTRA. The CFX

model comprised the complete BC system. The CFX results served to improve pool stratification models in SPECTRA. A coupled CFX/COCOCSYS full scope calculation was done for one phase of test BC4 in order to demonstrate an alternative simulation method in comparison to full CFD analysis and for demonstration of time and cost saving.

B.2Passive Safety Features Assessment and Optimisation (WP2)

This work-package served to investigate several open questions on the performance of the ESBWR Passive Containment Cooling System (PCCS) and possible improvements of the design. Integral system tests have been performed in the PANDA facility, aimed to assess the impact of hydrogen on the performance of the PCCS. This included interactions with drywell, wetwell and suppression pool. In the tests helium is used as the substitute for hydrogen. Two tests aimed to investigate the performance of the DGRS, a new design feature that can mitigate accident consequences and has the potential to provide safety and cost advantages in plant design. The PANDA instrumentation has been upgraded in order the to get detailed data about temperature and gas concentrations in the Drywell (DW) to satisfy the requirements for CFD code validation,. The test matrix has been based on ESBWR accident scenarios. The initial test and boundary conditions were defined in cooperation with the reactor vender (GE). The tests provided data on gas space mixing and stratification for code validation. To enhance the understanding of the experiments, representative tests have been analysed using GOTHIC, a containment code with 3D capabilities. The measured distribution of non-condensable gases and steam in the DW has been simulated with the CFD codes CFX and STAR-CD. The behaviour of the Passive Containment Condensers (PCC) in the presence of light gas has been studied by means of the two CFD codes CFX and FLUENT.

B.3Wetwell Gas Space Modelling and Performance Assessment (WP3)

Accurate prediction of containment pressure transients during severe accidents requires capabilities for 3D modelling of natural convection; mixing and stratification of multi-component gases, and condensation as well. These modelling capabilities must be reliable, validated and suitable for the nuclear engineering practice. WP3 is devoted to the validation of CFD models by performing medium scale tests in the KALI facility. The instrumentation has been enhanced in order to measure the local and instantaneous concentrations of the various species and the local temperature during the injection tests. Scooping calculations with the GOTHIC code provided guidelines for the positioning of instruments and for preparation of the test matrix. The KALI separate-effect tests consist in providing gas temperature and concentration spatial distribution during a transient in which hydrogen (or helium) and a steam mixture are injected into a closed vessel. In addition, the validity of the assumption that helium is appropriate to simulate hydrogen has been assessed. The test conditions were defined, to get the same main parameters characterizing the flow structures in the wetwell during the integral system tests performed in PANDA. KALI tests have been interpreted with the CFD codes STAR-CD and CFX and with the 3D containment code GOTHIC.

B.4Plant Evaluation (WP4)

This work-package served to integrate the results of the project and to translate those to the plant level. Two designs are considered: the ESBWR and the SWR1000. Concerning the ESBWR, the impact of the results of this project on potential containment simplification and plant safety has been assessed. The improved and validated models that resulted from this project are expected to allow a more accurate containment pressure calculation. Concerning the SWR1000, one severe accident scenario relevant for assessing the BC has been analysed in order to demonstrate the simulation capability of the validated models. A core melt scenario

after a stuck open safety valve accident was selected for analysis. The necessary plant and system data of the SWR1000 and the mass and energy release rates for the scenario have been provided. Full-scale calculations of the complete multi-compartment containment with a complete BC design were performed with the LP-codes SPECTRA and WAVCO.

C. WORK PERFORMED AND RESULTS

C.1 Validation of Building Condenser System Models

A number of computer code simulations of the SWR1000 Building Condenser experiment BC4 were carried out. The capabilities of the different codes have been compared and some guidelines and recommendations for the code users are provided.

C.1.1 SWR1000 Building Condenser PANDA Test BC4

Test BC4 was part of a series of tests performed in the PANDA facility at PSI [4]. BC4 is aimed to simulate the behaviour of the SWR1000 containment with Building Condensers (BC) under accident conditions. BC4 starts during the blow-down phase, 6 minutes after scram, for the case of a small leak in the upper part of the RPV and non-operation of the core flooding system. BC4 lasts until all water in the dryer/separator storage pool has been at about 100 °C. Figure 1 shows the PANDA configuration used for test BC4. During the blow-down phase, steam flows from the RPV into the DW and causes pressure and temperature to rise quickly. Due to the relatively high elevation of the leak, the temperature in the DW is stratified and air remains in the lower part of the DW, instead to be purged to the WW. The DW conditions at about 6 minutes after scram were estimated to be about 1.3 bar and 100 °C. These are the initial conditions for test BC4. After the end of the blow-down, due to BC operation and while the heat removed from the RPV by the emergency condenser and the SRVs only heats up the core flooding pool, the DW temperature decreases together with the pressure. At about 90 minutes after scram, and for about one hour, additional steam is produced when water from the core flooding pool is supplied to the DW and heated up through heat release from the RPV. The resulting power is a combination of the decay heat, additional steam production, and the heat-up of the core flooding pool. At about 3 hours SWR 1000 time, the core flooding pool no longer stores heat released by the emergency condenser or through the SRVs, and the amount of steam produced by the boiling pool corresponds roughly to the actual decay heat power. At about 5 hours SWR1000 time water starts to react with zirconium and, for about 4 hours, these chemical reaction leads to hydrogen release in the RPV, as well as heat release. Then, with increasing H2 concentration, the emergency condenser no longer removes any heat from the RPV and a steam-H2 gas mixture is vented to the core flooding pool through the SRVs. The zirconium-water reactions last about 4 hours, and when almost all the H2 has been vented to the DW the steam production corresponds approximately to the decay heat power. The test scenario is divided in four phases (Figure 2). BC4 starts with the simulation of the end of the blow-down to investigate the BC system response. BC4 continues with a second phase, simulating the pressure drop resulting from BC heat removal. During the third test phase, the RPV heating power is incremented regularly to simulate the increasing boiling rate of the core flooding pool, and the additional steam production when water from the core flooding pool is supplied to the DW and heated up through heat release from the RPV. At the end of the third phase, the RPV heating power is automatically controlled to simulate the decay heat power. During the fourth phase, He is injected into the RPV to simulate H2 release, and the heating power is incremented to simulate the heat release by chemical reaction. This fourth test phase lasts until the dryer-separator storage pool reaches saturation. BC4 lasted about 4 hours, corresponding to roughly 23 hours SWR1000 time.

C.1.2 Simulations of PANDA Test BC4 with Different Codes

COCOSYS Simulations

The first analysis for the test BC4 with COCOSYS, reported in [5] was successful, but showed some discrepancies in the results, which in turn became the reason for model changes. The improvements of a second analysis consist in an increase of subdivisions in the LP nodalization in DW2 and WW. The BC is now simulated with five subsequent tube zones similar to the BC3-analysis [6]. The secondary side of the BC is included in the COCOSYS model. The computational model for COCOSYS consists of 168 zones, 540 junctions and 137 heat absorbing structures. There is a 2-zone nodalization of the PCC-pool only. For the simulation of the water convection between the hot and cold part of the pool-water and the BC convection flow, pumps are interconnected. The simulation of the convection processes in the pool and BC by pumps was determined by iterative fitting to the test values. There is a detailed nodalization of the two DW- and the two WW-vessels. Here, special attention is paid to the DW1. Since the BC is installed in the upper part of DW1, the BC is subdivided into five pipe zones each lying in a separate DW1 zone. DW1 has a 9-level subdivision with about eight zones per level. The DW2 is subdivided with 9 levels and 4 zones per level. There is also a 9-level subdivision of the two WW vessels with 21 normal zones and three "water zones“. The COCOSYS heat transfer models at the inner side consider free- and forced-convection, as well as total radiation and a structure covered with water. If the water film evaporates there, the drain-wall model switches over to normal condensation mode. At the outer side of the insulated vessels, i.e. inside the PANDA building, total radiation and free convection is considered. The BC is axially modelled with five similar individual pipe zones and the same number of structures, using the same heat transfer models as for the other structures. A constant heat transfer coefficient of 1000 W/m^2K is used for the structures in the water zones of the WW. To simulate the direct heat loss through the steel support skirt from the DW bottoms to the WW domes special heat slabs were inserted.

WAVCO Simulations

The PANDA test BC4 has been simulated with WAVCO [7]. The pressure evolution during the PANDA BC4 test is determined by the condensation of steam in the WW and on the building condenser. As these processes depend strongly upon the steam concentration in the gaseous atmosphere, the simulation of the convective flow in the vessels and the mixing of the different gas components is of great importance. This includes especially the helium injected into the facility, replacing the hydrogen that is released from the primary circuit during a postulated severe accident in the SWR1000. Because of its low density helium may accumulate in the upper part of the vessels, hampering the condensation of steam on the building condenser. In general, increasing the number of cells in the numerical model for such a simulation improves the quality of the results. On the other hand the necessary amount of computing time rises considerably with the number of nodes. Therefore a reasonable compromise must be found, optimizing the ratio between the accuracy of the simulation and the expenses of the calculations.

GASFLOW Simulations

GASFLOW has been used to simulate containment phenomena of test BC4 to validate the modelling of mixing, stratification and condensation implemented in the code [8]. The He-Injection Phase has been simulated. This is the most challenging phase, because the presence of He limits the BC heat removal performance and accumulates in the DW. In GASFLOW the sources are defined as so-called internal sources, each of them occupying whole numerical cells. The original 45° inclination of the source in DW1 is modelled by means of two separate sources. One provides an inflow in negative vertical direction, the other an inflow in negative

radial direction. The addition of both vectors results in a 45° angle. However, test calculations have shown that the momentum of this source could not be resolved. The use of two cell volumes as a source causes an artificial widening of the jet, and hence a corresponding loss of momentum. The solution for this problem could be either a much finer resolution of the grid, which then will result in an inadequate computation time, or a reposition of the source to better represent its momentum. In order to study the influence of the momentum of the relocated source on the overall flow pattern in the DWs, a parametric study has been performed using two different source locations. The results support the hypothesis that the momentum of the source prevents the development of stratification at the BC and leads to a mixed atmosphere. The first new location is called the "reflecting position" i.e. the source is now in the position where the 45° inclined jet would be reflected by the bottom wall/pool water surface of DW1. Closer to the centreline, the cells are smaller and provide a smaller cell face area. Since the mass flow rate of the source is constant, a smaller cell face area results in a higher velocity of the jet, hence keeping a higher momentum. The highest momentum can be achieved by injecting the mixture of steam and helium through a source pointing upward. At the start of the He-injection phase, a slightly superheated mixture of He and steam flows into the DW1. The standard k-e-model has been applied to the whole computational domain. For condensation, the Chilton-Colburn analogy is used. The heat sink has a time-dependent surface temperature being applied from the temperature readings of the BC4 experiments. As a first approach, the measured water temperatures of the secondary (pool) side of the BC are set to be the actual surface temperature assuming an infinite heat conduction. A parametric study performed with two sources showed the influence of the jet momentum on the overall flow pattern and the pressure in the vessels. A low-momentum source pointing in a 45° inclined direction into DW1 has been used in the first simulation, a high-momentum source at the same position, just pointing vertically upward, in the second. The results are very different: In the simulation with the low-momentum source, the code predicts a too high system pressure (0.6 bar) and additionally the development of a strong temperature- and helium stratification in DW1 where the BC is located. With the high-momentum source, the atmosphere is better mixed in DW1 resulting in an over-prediction of the system pressure by only 0.2 bar at the end of the He-injection phase. With the low-momentum source, GASFLOW calculates a condensation rate which is generally too low. The high-momentum source shows a much better agreement. The momentum of the source has also a strong influence on the He-distribution in the PANDA vessels. More helium is stored in the WW in case of a low-momentum source resulting in a higher system pressure (Figure 3). The mass of He in DW2 is almost constant. The GASFLOW predictions of the temperature evolution in DW2 qualitatively agrees with the measurements, especially the temperature inversion is very well predicted. The He mass fraction vs. time, show that cold, but He-rich gas accumulates under the top of DW2 whereas warm, but He-lean gas is trapped in the lower part of the vessel. The upper volume is quite well mixed, whereas the lower one shows a small stratification of about 2 w% between the lowermost temperature sensors. The concentration difference between the upper and the lower volume amounts to 5 w%. Summarizing, the high-momentum source prevents the development of stratification at the BC in DW1. The atmosphere is quite well mixed which agrees with the test data. GASFLOW slightly over-predicts system pressure, but matches the BC heat removal due to condensation quite well. In the beginning of the He-injection phase, the condensation rate and hence the power removal is too high because the initial conditions don't match the real conditions of the experiment. Therefore, the temperature on DW1 is predicted roughly 5 °C too low. Test BC4 is simulated quite well with GASFLOW in the case of a high-momentum source.

CFX/SPECTRA Simulations

The objective of the CFX/SPECTRA BC4 simulation was to demonstrate and validate the use of a coupled CFD/LP code approach for performing a full scope accident simulation of a nuclear power plant. "Full scope" refers here to the whole plant being modelled, including RPV, containment, safety systems, reactor building, and environment. The analyses of test BC4 concentrated on thermal stratification of the BC pool and gas stratification in the space around the BC unit, both with respect to their influence on the long-term containment pressure. It is well known that system codes based on LP approach are inherently unable to predict stratification, whereas CFD codes are in theory applicable for this purpose. However, CFD codes suffer from long computational times for typical accident transients, even when applied to computational domains encompassing a single or a few compartments, and for this reason are unsuitable for system analyses. Therefore, a three-step, combined procedure was followed, taking benefit of the strong points of both approaches: Step 1 consists of a full scope analysis using the system code SPECTRA. In step 2, CFD analyses of the selected parts of the system are performed with CFX. Step 3 consists of an updated full scope analyses with SPECTRA, using CFD results to improve SPECTRA model.

For the CFD computations of the BC pool, a 3D model of the pool was developed. The flow domain consists of a turbulent region, separated from a laminar region due to stratification. Both the standard k-ε turbulence model as well as a low Reynolds k-ε turbulence model have been used in the analyses. For the computation with the standard k-ε turbulence model, a mesh consisting of 565.000 cells has been used. Subsequently, this mesh has been refined near the walls. The resulting second mesh consists of 754.000 cells. This mesh has been used for the computation with the low Reynolds k-ε turbulence model. Since the analyses have been performed up to the time where transition to two-phase flow takes place, the analyses were done in single-phase. The CFD computations of the DWs have been performed with CFX-4.4. The grid of the two DWs consists of 620.000 cells. The gas mixture in the DWs is modelled as a multi-component mixture consisting of steam, helium and air. A compressible flow model was applied. In the transient computations, an automatic time stepping procedure has been used. The wall condensation model developed by NRG was applied. Condensat is removed from the computational domain. Since the pool at the bottom of the DWs has not been modelled, the problem is reduced to a single-phase problem. SPECTRA was applied for the full scope analyses. The model consists of 12 control volumes, 19 junctions, and 10 solid heat conductors. All pipes connecting the two DWs and the two WWs were modelled using two parallel junctions, representing the lower and the upper part of the connection respectively. This allows for counter-current flow and mixing of fluids from the two connected volumes.

Validation of the CFD Model of the BC Pool: In order to calculate the BC pool water outlet temperature correctly, it is essential that mixing in the BC pool is predicted accurately. The outlet temperature as predicted by the standard k-ε model is significantly higher than the measured value. This is caused by the over-prediction of mixing in combined turbulent-laminar stratified flows by the standard k-ε model. It was concluded that mixing cannot be computed accurately with this model for flows including stratification/relaminarization. Phenomenological, the flow in the BC pool consists of two regions, created by the sparger which produces an unstable velocity field in the pool (shown in Figure 4). This velocity field results in good turbulent mixing in the upper part of the pool. However, the lower, cold part remains stratified during the considered transient time [9].

Validation and Application of the CFD Model of the DWs: The BC4 transient was calculated during the He-injection phase. The gas flow injected into DW1 consisted of about 15 mass% He and about 85 mass% steam. The computed system pressure corresponds almost

exactly to the measured value during the He-injection phase. The effect of the system temperature on the pressure is limited to a few percent. The amount of steam and helium present in the DWs is predicted within a few percent. Helium and steam flow rates from DW1 to the WW are also calculated within a few percent. The condensation rate of steam at the BC and at the walls of both DWs is predicted within 25%. The CFD simulation proved in particular useful to understand the helium distribution inside both DW volumes during the test. Due to condensation of steam, the He mass fraction in DW1 increases steadily from zero to a maximum of about 0.4 at 8000 s. At this time the He concentration in DW1 starts to decrease due to the injection of pure steam into DW1. Helium and steam are mixed homogeneously in DW1 during the helium injection phase due to the strong re-circulation flow pattern that takes place in DW1. He is transported from DW1 to DW2 via the upper half of the large interconnecting pipe. Inside DW2, this transported helium gas starts to rise directly due to buoyancy. The induced flow results in well mixed conditions above the stratification front [10].

Improved Pressure Prediction with the SPECTRA/CFD Model: SPECTRA analyses of the BC4 test were performed in order to determine the sensitivity of containment end pressure to stratification in DWs and the BC pool, prior to the combined LP/CFD code analysis. The effect of thermal stratification of the BC pool on containment end pressure was investigated in calculations with various stratification models for the pool, including the perfectly mixed BC pool. The SPECTRA internal stratification model, as well as the values obtained from CFD analysis of the BC pool were applied. It was concluded that, as far as the containment parameters were concerned, there was practically no influence of BC pool stratification on the results. The effect of stratification in both DWs and the RPV on containment end pressure was determined by varying the level of stratification in these volumes. The results showed a significant influence of gas stratification on containment pressure, with the calculated end-pressures varying between 4.8 and 5.4 bar. Based on this, it was concluded that calculation of the stratification in the DWs with CFD would be useful. The SPECTRA analyses also showed that the performance of the BC unit was rather similar in all cases. This was caused by the self-adapting property of the system. It is therefore concluded that it is not necessary to create a detailed model of the BC unit within the CFD code. A simple BC model, involving boundary heat flux and condensation rate prescribed based on SPECTRA calculations should be sufficient. The detailed results of calculations performed within a combined LP/CFD code analysis are given in [11]. The overestimation of pressure in the Step 1 calculation is characteristic of all system code calculations of the BC4 test. Stable stratification of DW2 is accompanied by stable trapping of helium in this volume. With perfect mixing of DW2 as assumed in system codes, less helium is trapped in DW2. However, DW1 does not keep the helium, which is instead transported through the overflow pipe to the WWs. Consequently, the amount of helium present in the WWs is clearly smaller in case of a stratified DW2 than in case of a perfectly mixed DW2. Since the WW pressure is the back-pressure of the system, the amount of helium ending up in the WW determines the system end pressure.

Main conclusions: As far as the containment parameters were concerned, there is practically no influence of BC pool stratification on the results. The combined SPECTRA/CFX approach to passive containment modelling applied to test BC4 resulted in a best-estimate value for the calculated containment end pressure, within measurement accuracy of the experimentally observed value of 4.7 bar. Sensitivity analyses of the BC4 test with respect to stratification in gas spaces showed a worst case value of 5.4 bar. This value should be adopted in a bounding analysis. It would translate into 0.7 bar or 15% containment pressure margin.

STAR-CD Simulations

The simulation with the CFD code STAR-CD was focused on gas mixing in DW1 of test BC4 during the He-injection phase [12]. The code predicts the transient formation of a buoyant

jet, which extends from the source up to the top of the DW. The jet contributes to stratification near and above the BC elevation. However, the predicted stratification is not strong enough compared to the experiment and the analysis of the BC performance during the steam injection phase will demand a special development as far as no condensation model is yet available in STAR-CD. Even if not completely realistic, a simplified 2D modelling has shown to be useful to initiate some local sensitivity studies, especially in the zones of jet impingement and of mixing around the BC location. Before selecting 3D modelling, this 2D geometry is also an opportunity to test some specific models for diffusion, condensation and turbulence. As far as 3D modelling is concerned, the feasibility has been demonstrated that STAR-CD is capable to predict mixing and, at least partially, stratification patterns in DW1. From both 2D and 3D calculations it can be concluded that during the He-injection phase, the temperature evolution in DW1 is correctly predicted and that the steam injection phase reveals a need to improve the BC representation. The continuation of theses simulations will be devoted to 3D transient analysis. The first attempts with refined 3D models have shown that the time of response is about one week for a 1000 s transient, which corresponds to almost one month for both phases of He and steam injection analysis. Therefore, these models are not convenient for parametric studies contrary to LP codes, all the more as a coarser mesh is not always relevant. The development of new subroutines is needed to better model the heat and mass sink induced by the BC and the feed line, as well as another subroutine for local gas injection at a prescribed rate in a specified cell. Looking to future 3D calculations, two tentative approaches were done and have shown promising. These concern first a coupling of 3D steady-state/3D transient calculations. Following this strategy, the final temperature field in DW1 after the He-injection phase is evaluated through a steady-state analysis, then the results are used as initial conditions for a subsequent transient analysis of the steam injection phase. In the second approach a model with DW1 only was used for the analysis of the steam injection phase, considering that the flow to DW2 is very weak and does not affect the BC performance. It might be very cost effective to examine the flow distribution in a model with DW1 only, for conditions that will help to assess the future complete STAR-CD calculations. The results obtained are very promising.

C1.3Comparison of Code Performances and Guidelines

The capabilities of the different codes have been compared [13]. Simulations were done by traditional LP codes (WAVCO, SPECTRA, COCOSYS), but there is also one CFD code (GASFLOW) and a combined run involving CFX and SPECTRA. GASFLOW was not run over the full time of the test. Therefore, the error propagation is not be traced. Test data are used at the beginning of the entering point as initial conditions. A general impression is, that if there is good agreement with some data, this does not mean, that there is also good agreement with others. Apparently, not all quantities are coupled with each other, although the complexity of the experiment and the interconnection of the PANDA vessels may this imply. Some major data to be compared were selected. In Figure 5 the DW pressure is compared. There have been many attempts to simulate the pressure transient. A key feature of a simulation is a very good mixing in DW1 and stratification in DW2 to reach good agreement between code prediction and experiment. This target can be reached as most simulations show. For the He partial pressure the codes show considerable differences. The air partial pressure consequently also reveals differences in the time history. In DW2 there is a similar but less strong divergence of predictions. In Figure 6 the heat flow through the condenser is depicted. Three methods were used to determine the heat transfer. These are condensate flow measurement, energy balance of the dryer/separator storage pool and energy balance of the BC pool. GASFLOW data are only available for a short time and show some overshoot when the simulation starts. COCOSYS data are in good agreement but produced by the help of some experimental data for representation of the secondary side. SPECTRA under-predicts the power in the initial phase, when sub-cooled

water flows through the BC tubes. Since the water mass flow rate through the tubes is well predicted, this is probably caused by too low heat transfer coefficient on the water side during low flow phase. WAVCO shows good agreement in the beginning but later under-estimates the heat flow. In summary, all codes appear to be able to simulate the characteristic behavior of the BC satisfactorily and most codes were able to provide good predictions.

The current situation and level of code development, discussed in some detail for test BC4, can be characterized as follows: Only LP codes appear to be able to provide comprehensive predictions for a complex, long time experiment like BC4. CFD codes due to limitations, still existing in the modeled physics and available computer resources, are either restricted to simulate selected periods in time or to include only parts of the problem. CFD codes are also used to support LP codes (combination of CFX–SPECTRA) in understanding special situations or to provide additional information in particular for all phenomena related to momentum exchange. LP codes have limitations whenever flow dominates the processes under investigation. A good example is the mixing in DW1 and DW2. Here the use of CFD enabled an LP code to improve the modeling of mixing in order to obtain more realistic predictions. The integral experiments conducted at the PANDA facility have proved to be a challenge to simulation by computer codes. In view of up-scaling to full size geometries found in a containment and running in blind mode, code application and development should take into consideration the following. CFD codes will become able to simulate long-term processes with increasing computer power and/or parallelization. Fast running and robust solver algorithms are necessary to be implemented. The complexity of the physics, addressed by experiments like BC4, calls for the implementation of additional models in CFD codes as a standard feature. Among these are wall condensation, simplified heat conduction and sump modeling. Furthermore, the codes have to be able to run the physical models in combination with each other. Almost each experiment involves special features (building condenser), which have to be simplified somehow. Codes must be able to allow users to implement easily user-models and additional coding. Also for LP codes is applicable, that models for specific phenomena may be missing. Depending on the code this can be simulation of pure water volumes, improvements in the BC heat transfer models or condensate treatment involving sump modeling. LP codes have clear limitations with processes, which involve momentum dominated transport. In these cases the use of CFD codes is recommended. A recommended trend could be, to use LP models to get an overview of a scenario and to conduct parametric investigations. CFD codes can be applied for specific and more detailed investigations, identified by previous LP runs. Alternatively, coupled approaches between LP and CFD to split the computational region or improve the depth of modeling in an overlapping set-up could be introduced.

C.2 Passive Safety Features Assessment and Optimisation

Several aspects of passive safety features response on hypothetical LOCAs, including BDBAs with hydrogen release, have been studied. Important goals were to better understand the relevant phenomena that occur in passive systems and to further improve computer codes with 3D capabilities. New integral system tests related to the ESBWR have been performed in the PANDA facility. The tests were aimed to assess the impact of hydrogen on the performance of PCCS and containment. Two tests were aimed to investigate the Drywell Gas Re-circulation System (DGRS), a new design feature that can mitigate accident consequences. The tests have been analysed using GOTHIC, a containment code with 3D capabilities. The distribution of non-condensable gases and steam observed in the tests has been simulated with CFD codes (CFX and STAR-CD). The behaviour of the Passive Containment Condensers (PCC) has been studied by means of two CFD codes (CFX, FLUENT).

C.2.1 Integral System Test Programme in PANDA

The containment behaviour of the ESBWR in case of an accident has been experimentally investigated in PANDA. Five integral system tests were performed to study the long-term cooling phase following a postulated LOCA. In addition the effect of hydrogen release in case of core over-heat was investigated [14]. The focus of the tests was on the following aspects:

- Impact of light gas on PCCS performance (Test T1.1);
- Influence of mixing/stratification on PCCS and containment behaviour (Test T1.2);
- Significance of additional heat release due to metal-water reaction on PCCS and containment behaviour (Test T1.3);
- Performance of DGRS in reducing long-term containment pressure in case of an accident with H2 release (Test 2.1), and without H2 release (Test 2.2).

A comparison between ESBWR and PANDA facility is shown in Figure 7. The 1390 MWe ESBWR [3] is an evolution of the 670 MWe SBWR [15], designed by General Electric (GE). Both concepts make use of passive systems. These systems provide emergency core cooling, keep the reactor core cooled and remove decay heat from containment. The systems performing these tasks are the Gravity Driven Cooling System, the Isolation Condenser System, and the Passive Containment Cooling System (PCCS). The large-scale thermal-hydraulic PANDA facility allows for investigating LWR system behaviour and containment phenomena [16]. PANDA was first used to study passive decay heat removal systems and containment response of the SBWR. Later, system tests were performed for ESBWR and SWR1000. PANDA was used again for the projects NACUSP (Natural circulation stability in BWRs) and TEMPEST.

Test Specification, Initial and Boundary Conditions

Test T1.1 (Base Case) investigated the impact of light gas on the PCCS and containment performance in case of a MSLB LOCA and release of large amounts of light gas caused by core overheat later in the transient. According to the test configuration (shown in Figure 8) the RPV is connected to both DWs to equally distribute the break flow to DW1 and DW2. All three PCCs are available. Hydrogen release is simulated by injecting helium into the two break flow lines, going from the RPV to the DWs. He-injection started at 10000 s after test initiation for a period of two hours. The test is to provide data on PCCS performance in the presence of light gas and on gas space mixing/stratification in the DWs.

Test T1.2 (Stand-by Volume) investigates how light gas affects PCCS and containment behaviour in a very special test configuration (Figure 8) where DW1 is acting as a large stand-by volume. The total break flow goes to DW2. Only PCC2 and PCC3 connected to DW2 are used. Helium injection to the DW2 is initiated at 10000 s after test initiation for two hours. This test is to provide data about accumulation of non-condensable gas in the DW2 dead-end volume and on gas space mixing/stratification.

Test T1.3 (Asymmetric Case) is aimed to assess the effect of light gas and additional heat release due to metal-water (M-W) reaction on PCCS and containment performance in a special (asymmetric) facility configuration (Figure 8). The total break flow goes to DW1. Only PCC2 and PCC3 connected to DW2 are used. He-injection to the DW1 is initiated at 10000 s after test initiation for two hours. During He-injection the RPV heater power is increased in order to simulate additional heat release caused by M-W reaction. This test provides data on gas distribution in a very special configuration and on system behaviour under BDBA conditions.

Test T2.1 (Base Case with DGRS) is to assess the combined PCCS and DGRS performance when light gas is injected. The test configuration is the same as for the Base Case Test T1.1 (Figure 8). The DGRS is activated at 10000 s after test initiation, when He-injection starts, and run until the end of test. The test provides data on gas distribution and on PCCS performance in the presence of light gas and on the performance of the DGRS in retaining non-condensable gas in the DW, thereby reducing long-term containment pressure.

Test T2.2 (Base Case with DGRS, no He-release) is to assess the combined PCCS and DGRS performance in case of an MSLB LOCA with no hydrogen release. The test configuration is the same as for test T2.1 but no helium is injected and the DGRS is activated at about 21600 s after test initiation. The test provides data on the performance of the DGRS in retaining gas in the DW that is heavier than steam (air).

The initial conditions are the same for all tests and correspond to the plant status predicted by TRACG for the ESBWR at one hour after scram, triggered by an MSLB-LOCA. At this time DW conditions are at 2.5 bar / 127 °C. The heater power in the PANDA RPV is controlled to match the scaled (1:40) decay heat release. The power was 1276 kW at test begin and decreased to 638 kW at the end of the 12 hours tests. For tests with only two PCCs available the power is accordingly reduced. In test T1.3 the power is increased during He-injection to simulate additional heat release caused by M-W reaction. The equivalent mass of He for simulating H2 release was assessed based on the ESBWR design and assuming 100% cladding M-W reaction. The gas re-circulation flow rate of the DGRS is based on a parametric study performed by GE.

PANDA Experimental Results

The tests are characterized by three phases showing generally the following typical behaviour:

Phase 1 (before He-injection starts): The PCCS started working immediately after test start. The PCCs were slightly over-loaded and, therefore, not able to remove all heat released from the RPV. Therefore, a steam/air mixture was vented from the DW to the WW for the first 20 minutes. Within the first hour into the test all residual air in the DW was vented to the WW gas space. The venting process leads to an increase in WW pressure, and with it also the DW pressure slightly increased in the very beginning of Phase 1 (Figure 9). After all the air was purged to the WW, the pressure in DW and RPV decreased slowly, in accordance with the decreasing decay heat power and, therefore, increasing over-capacity of the PCCs.

Phase 2 (during He-injection): As soon as He-injection started, the system behaviour significantly changed. Helium release caused a continuous increase in system pressure (Figure 9). An increase in WW pressure is observed because of almost continuous venting from the DW to the WW, through the PCC vent lines. During this phase the PCC heat removal capability was degraded by the non-condensable gas, which flows together with steam from the DW to the condensers. The degradation is reflected in the reduced condensate flow returning to the RPV.

Phase 3 (after completion of He-injection): As shown in Figure 9, the system pressure kept on increasing for about 3000 s after He-injection stopped. At around 20000 s into the tests, when almost all helium has been purged from the DW to the WW, the PCC performance recovered and a kind of new equilibrium was established between heat removal capability and actual decay heat release. Consequently, the pressure stabilized at higher level and later slowly decreased until the end of test. The pressure level finally reached in the DW is mainly determined by the amount of light gas released during the course of the accident.

Observations about mixing and stratification in the Drywell: The tests performed in different facility configurations showed a variety of mixing/stratification patterns. The results for the Stand-by Volume Test T1.2 are shown in Figure 10. Helium accumulated first in DW2 to finally reached its maximum concentration of 30% at the end of the injection phase. Shortly after He-injection started He also flowed to DW1 (stand-by volume). In the upper region of DW1 the helium concentration reached 31% at the end of injection and increased further to 42% to the end of test. In the lower region of DW1 the helium concentration decreased after injection stopped and approached about zero at the end of test. In DW2 the helium concentration reached about the same level as in DW1 at the end of the injection phase but no helium could be detected in DW2 about 4000 s later.

Observations about PCC Behaviour: The PCC behaviour was largely changing during the course of the tests. Before He-injection, PCC heat removal was in equilibrium with the decay heat release. During the injection phase the PCCs removed less energy from the DW because condensation was degraded by non-condensable gas. Based on measured gas temperatures in the upper and lower drums of the condenser and in the central tube different operation modes of the condenser have been observed during the course of a transient. Figure 11 shows for test T1.1 the measured vertical gas temperature profiles, from the upper header through the central tube down to the lower header, for three different transient times: at 3500 s (before He-injection), at 12500 s (during He-release) and at 29000 s (after He-release). Before He-injection, a mixture of steam and small amounts of air is supplied to the PCC upper header and passed downwards through the condenser tubes. In this phase, temperature measurements indicate two separate zones (Figure 11, t=3500 s). In the upper zone steam is condensing at saturation temperature. In the lower zone a mixture with air and relatively low steam content is accumulating. Here, the gas temperature approaches the PCC pool temperature of about 100 °C.

The boundary between the two zones is moving upwards during the test because the PCCs adjust their heat removal capacity to the actual decay heat release by progressively accumulating air in the lower part, thereby reducing the effective condensing area. If not sufficient air is available for blanketing enough heat transfer area, then PCC over-capacity results and the DW pressure starts to decrease. After initiation of He-injection the PCC operation mode changed significantly. In presence of gas that is lighter than steam, buoyant forces, arising from steam condensation out of a steam/He mixture, strongly influence the flow patterns inside the PCCs. The clear separation into two zones described above disappeared and a different vertical temperature gradient is established along the tubes. Two different operation modes could be identified: The first mode refers to a situation in which a vertical temperature gradient showing higher temperature in the top and lower temperature in the bottom is observed. This indicates that the steam/helium mixture is flowing downwards in the tube and is becoming more and more helium rich as condensation proceeds This first mode was observed in PCC3 in test T1.1 from the beginning of He-injection till t=23500 s into the test (Figure 11, t=12500 s)). The second mode refers to the situation in which the temperature levels in the upper and lower drums are maintained, while a reverse temperature gradient is established. The gas in the tube is colder than in the lower drum, indicating that the flow was re-circulating upwards and again becomes colder due to steam condensation (Figure 11, t=29000 s). The PCC flow patterns proved to be much more complex for steam/helium mixtures than for steam/air mixtures.

Effect of DGRS on System Response: Test T2.1 demonstrated that the DGRS is able to retain non-condensable gas in the DW. As can be seen from Figure 4.2.6 the resulting DW pressure (peak and long-term) is about 0.3 bar lower for the test with DGRS activated (T2.1) compared to the test with same conditions but without DGRS (T1.1). At the end of test T2.1 the DGRS was stopped to simulate a failure of the system. The pressures in DW and WW

immediately started to rise and after 30 minutes approached the same level as measured for test T1.1 (with no DGRS). Non-condensable gas is only retained in the DW as long as the DGRS is working. It appears that the amount of gas retained in the DW depends also on the configuration adopted for the DGRS piping, i.e. the elevation where the re-circulation flow is re-introduced to the DW. In the current PANDA configuration the flow is injected at about mid-height of the DW. More volume would be available to store gas if the injection would be at the bottom of the DW. With respect to the ESBWR containment, the design of such a DGRS system should be optimised accordingly.

Conclusions on PANDA Tests: The containment behaviour of the ESBWR in case of a LOCA, including the effect of core over heat with release of hydrogen has been experimentally investigated [17 to 23]. An extensive database for model validation and code qualification has been produced. All tests showed a similar behaviour of containment and PCCS before He release. During He-injection the system pressure increased rapidly, mainly because of the added gas and only to a minor degree because of degradation in PCC performance. Some time after He-injection stopped and no more gas was vented from DW to WW, the PCC performance recovered and the system pressure finally stabilized at higher level. Although during He-injection PCCS performance was degraded, no significant energy deposition occurred in the WW. The tests clearly showed that the PCC operation mode is significantly different for steam/helium mixtures and steam/air mixtures. The tests helped to better understand the PCC behaviour in the presence of light gas. Nevertheless, new tests with further upgraded instrumentation could provide more insight to the complex flow patterns. The DGRS showed its capability to retain non-condensable gas in the DW, thereby slightly reducing containment pressure. A disadvantage is that in case of a failure the containment pressure raises quickly to the level without DGRS.

C.2.2 Analytical Investigations

Simulation of Helium Distribution and Condensation in Drywell

Calculations with GOTHIC

The PANDA tests provided a unique database for the assessment of the capabilities of the GOTHIC code. The stratification patterns produced during the tests with helium in the two DWs covered a variety of conditions and controlling phenomena, which put in evidence the merits of a 3D modelling of large, connected volumes. The experiments provided conditions to test the limitations of the code, as well as of the necessarily coarse mesh used for the long transients investigated. The tests have been analysed, using both, LP and 3D representations of the DWs. The focus was on prediction of gas distribution in DWs, and its effect on the pressurisation of the system. Post-test simulations for test T2.1 with DGRS and the stand-by volume tests T1.2 have been performed. A mesh sensitivity study was conducted for test T1.2 to verify the modelling detail required to capture strong stratifications. In view of the results obtained [24], the most interesting conclusions should refer to the effect of gas distribution on system response and to the prediction of local gas accumulation phenomena.

In general, the coarse meshes used are capable to capture most of the stratification patterns observed in the test. The predictions with the 3D model were always closer to the test data than those obtained with the LP representation of the DWs for all the conditions where the in homogeneity of the gas distribution had a mitigating effect on the pressure build-up. Figure 12 shows the comparison between the experimental pressure in Test T1.3 and the results calculated with the LP model and the 3D, coarse-mesh model. The retention of helium in regions of the DW and the purging rates from the regions where it accumulated were predicted fairly well, so that the effect of various configuration conditions (including effect of DGRS) on the final pressure could be simulated. A mesh sensitivity analysis was performed for the stand-

by volume Test T1.2, using a finer mesh representation of DW1. The model of both DWs consisted of about 10'000 cells. This sensitivity analysis revealed that the finer mesh would not necessarily be required for calculating the global transport of gas from the dead-end region (upper half of DW1) to the connected vessel and from there to the WW. No substantial difference in the pressure predicted with the two models could be observed, both computing a higher pressure than in the test. Figure 13 shows that the simulation with the coarse-mesh of the flow patterns in DW1 that are expected to have prevailed in the test, was quite reasonable, and reproduced the process of He accumulation in the upper part of DW1 during the second phase of the test. The insensitivity of the predictions to the quality of the mesh may be due to the low turbulent diffusivities calculated by the code for the low-flow conditions prevailing in DW1, which results in the prediction of strong concentration gradients even using a rather coarse mesh. As this feature seems to be peculiar of GOTHIC, these conclusions should not be applied to other CFD codes. As regards local accumulation phenomena, various interesting results could be obtained for Tests T1.2 and T1.3. Notably, the increasing He-concentration in the upper half of DW1 during Test T1.2 could only be predicted with the fine-mesh model, whereas a large discrepancy with the data was observed in the simulation with the coarse-mesh model. However, the dramatic improvement in the prediction of the He-concentration in DW1 obtained with the fine-mesh model produced a very minor effect on the prediction of the system pressure. The simulation of Test T1.3 performed with the coarse-mesh model, resulted in an inaccurate representation of the purging of helium form the upper part of DW1. These two results, as well as the incapability of the coarse-mesh model to predict cross-sectional distributions in various tests, showed that the prediction of local phenomena may require a very detailed mesh, probably finer than that which can be currently afforded with the available computer resources. This conclusion shows the limitations of the current capabilities. However, it indicates that detailed investigations with CFD codes (for instance to predict the build-up of local pockets of dangerous hydrogen-rich mixture in confined spaces) may become a required engineering tool to tackle the hydrogen risk problem in a complex geometry as soon as the progress in computer sciences will allow large-scale simulations.

Calculations with CFX

The objective of modelling Test T1.2 with CFX was to demonstrate and validate the capability of the code for predicting stratification in containment volumes. This fits well into an overall strategy of containment modelling, to apply system codes for full scope plant analyses, and CFD codes to calculate multi-dimensional phenomena. The CFX mesh of the two DWs consists of 788.500 cells. A finer mesh has been used for DW2, in which steam and helium are injected. Due to this injection, the gradients in the flow quantities in DW2 are larger than in DW1. A pool of water is present at the bottom of the two DWs, originating from condensation of steam. The gas mixture in the DWs consists of steam, helium, and air. For the transient calculations an automatic time stepping procedure has been used. Buoyancy is included. The flow is non-isothermal, with the enthalpy equation being solved in the CFD model. A mixed turbulent/laminar stratified flow occurs in DW1 during test. Mixing is over predicted using the standard k-ε turbulence model for this situation. In contrast, low Reynolds k-ε turbulence models are well capable of predicting mixing in combined turbulent/laminar stratified flows. However, these turbulence models require a much finer mesh density near the walls in order to resolve the boundary layers and are less stable than the standard k-ε turbulence model. Therefore, the computations have been performed using the standard k-ε turbulence model. A model for wall condensation is not available in CFX-4. Therefore, a model has been developed and implemented for calculating the steam condensation and for defining sinks of steam and enthalpy. The inlet mass flow rate, the corresponding temperature, and the helium mass fraction of the discharge flow into DW2 have been used as the inlet boundary conditions. A pressure

boundary was used at the outlets of the computational domain respectively at the PCC supply lines. The measured wall temperatures have been used as boundary conditions.

The CFX-4.4 model has been applied to calculate the He-injection phase of test T1.2, covering the period of 9,500 - 17,000 s [25]. It proved practically impossible to cover also the post-He-injection phase, due to the relatively slow convergence of the computation, which resulted in a net CPU time of three weeks for 7,500 s of transient time. The calculated mass fractions show that the He-distribution in DW2 during the transient is quite homogeneous, indicating well mixed conditions, as illustrated in Figure 14. DW2 is well mixed due to the strong re-circulation flow pattern generated by injection of helium and steam into DW2. The Figure also shows that helium is transported from DW2 to DW1 via the upper half of the interconnecting pipe. The helium entering DW1 rises directly due to buoyancy, resulting in stratification, with well mixed conditions above the stratification front. The front moves slightly downwards during the considered transient time. In the stratified DW1, the helium concentrations are predicted within 10% accuracy and the increase of gas temperatures is over predicted by 15-25%. In the well-mixed DW2, the helium concentrations are predicted within 10-15% accuracy, whereas the calculated gas temperatures increase is over predicted by 100%. It was not possible to retrieve the cause for the observed discrepancies.

Calculations with STAR-CD

For validation purposes of the CFD code STAR-CD 3.15 the tests T1.1 and T2.1 were selected. The tests provide challenging data for code analysis on accumulation of non-condensable gas and on mixing/stratification in the DWs. The modelling strategy used to represent the DWs results from previous PANDA simulations, where it showed to provide sufficiently accurate results in relation to mixing/stratification processes, even using a coarse mesh [12]. The model uses a uniformly spaced Cartesian coordinate system with 2976 cubic cells. The flow rate to the PCCs is represented by an outlet velocity profile and the walls of DW vessels are supposed to be adiabatic. Buoyancy-driven flows and natural convection are taken into account. The standard k-ε turbulence model "High Reynolds number" for the turbulence characteristics is used. Condensation is not taken into account. The time steps are constant and equal to 1 s.

Test T1.1 results: The detailed 3D-calculation is supposed to start at beginning of He-injection and to stop 15000 s later, after DW pressure stabilized. Before the PCCs start to operate, the DWs can be considered as two closed interconnected tanks. This constitutes a discrete fluid oscillator governed by compressibility, which may give rise to resonance-related fluctuating forces. In fact, the PCCs are operational and significantly change the system behaviour as soon as the He-injection begins. The containment pressure is mainly governed by the performance of PCCs and by the amount and transient distribution of non-condensable gases initially filling the containment or being released later in the transient from the reactor core. The DW pressure increases as long as He is injected and keeps on increasing for about 3000 s after the end of injection, both in the experiment and in the STAR-CD calculation. The highest pressure in the DW is approximately 5.6 bar in this test and 5.6 bar in the calculation. Containment temperatures are determined by gas distribution and pressure inside both DWs. As far as gas mixing in DW is concerned, right after the beginning of He-injection, helium is practically immediately well mixed with steam in the DW, than the measured temperatures evolve with time almost in the same ranges for both DWs. Despite the coarse grid, the general trend of the temperature profiles is satisfactorily predicted by STAR-CD, as well as the stratification patterns originating by symmetric injection conditions of test.

Test T2.1 results: Two phases are considered in the calculation: These are Phase 2 (during He-injection and DGRS activated) and Phase 3 (after He-injection and DGRS activated). In the zone of DGRS operation, the negative buoyancy-generated flow is clearly reproduced by the simulation, which also shows the entrainment induced by the strong buoyancy effects in both ends of the interconnecting pipe. The pressure history calculated with the 3D-model is nearly identical to the experimental evolution during phase 2, but the code over-predicts the pressure during phase 3. This major discrepancy does not seem to be related to compression of the gas, since the temperatures are not over-predicted in the same range. It might be due to some other effects that have not been included in the analysis. During phase 2, a vertical stratification of the measured temperature distribution appears in DW1 and DW2. As a consequence of the DGRS activation, the gas temperatures in the bottom of the DW increase faster than the temperatures in the top of the DW. The general trend of the temperature profiles in DW1 and DW2 is satisfactorily predicted by STR-CD. Test T2.1 has given a first insight into the PCCS performance and overall system behaviour in a postulated accident, during which a large amount of light gas was released to the DW and the DGRS was activated. The simulation has shown the difficulties to calculate gas mixing in a condition of double forced convection due to the injection jet and due to the DGRS. The pressure in the DW is overestimated by the code and no tentative has permitted to improve this situation without deteriorating estimation of other relevant variables. It seems that there should be a significant influence of the gas stratification on containment pressure. The positive point seems to be that the CFD modelling with coarse mesh is able to predict reasonable trends of the temperatures and to reproduce the He stratification patterns in the DWs [26].

PCC Performance Calculations

Nitrogen or air, or, in case of severe accident, hydrogen can be present in the PCCs of the ESBWR. The presence of non-condensable gas in steam can degrade condensation rate and heat transfer. The impact of light gas (H2 in reality, He in PANDA tests) on the PCC behaviour during test T1.2 has been analysed by CFD codes (CFX. FLUENT).

Calculations with CFX-4

The PCC behaviour was analysed with CFX-4, first to develop and to validate a CFD model for predicting the condensation rate of a PCC, second to analyse by means of the CFD model the phenomenology of the PCC in the presence of helium. The CFD model should be suitable for conditions typical of phase1 (injection of steam-only) and 2 (injection of He-steam mixture). During phase1, with steam-air atmosphere in DWs, PCC operation is characterized by steam condensation taking place in the upper region of tubes. Measured gas and tube wall temperatures drop to the pool level temperature in the lower region. During phase2, with sufficient helium present in the DWs, inversion of the temperature profile was observed in some of the PCC tubes, which is attributed to flow reversal in these tubes. During the He-injection phase, the response of PCC2 and PCC3 differ and also tubes within a single PCC behave differently, complicating prediction of PCC phenomenology.

The CFX model comprises one quarter of PCC geometry. Although the PCC actually is not fourfold symmetric, it is believed that the typical behaviour can be simulated with this model. The mesh consists of 143900 cells. A low Reynolds turbulence model would be best to predict the flow field in the PCC tubes, which is characterized by mixed laminar/turbulent flow with buoyancy effects. However, this model require a very fine mesh near the walls in order to resolve the boundary layers and is less stable than the standard k-ε turbulence models. Therefore, the standard k-ε turbulence model was applied. The wall condensation model developed by NRG was used. A constant film thickness at the tube walls was assumed, whereas in the experiment the film thickness increases with decreasing vertical position due to the

condensation of steam. The model has been validated against experiments. The CFD model did not allow for calculating the whole transient, due to the complex behaviour of the PCC. Instead three cases have been defined. Case 1 corresponds to the conditions at the end of phase1 at 10000 s. Cases 2A and 2B correspond to the conditions at 11000 s in phase2. The influence of the presence of He on PCC behaviour has been analysed by comparing the results of cases 2A and 2B with those of case 1 (with no He present in the system). In Case 2A the feed flow rate has been increased compared to the experimental value to a value where no flow reversal occurred. In Case 2B the actual experimental value has been prescribed. The effect of flow reversal on PCC performance could be investigated by comparison of Cases 2A and 2B [27].
Case 1: The calculated condensation rate of one PCC is in good agreement with the test. Note that a high condensation rate is accompanied by a large temperature difference across film and tubes. The required removal of condensation heat is limiting the condensation rate. The calculated tube wall temperature distribution agrees qualitatively well with the experiment.
Case 2A: The driving force for steam condensation (partial steam pressure difference between bulk and film) decreases with respect to Case 1, because of the presence of He. Therefore, the calculated steam condensation rate decreases by 32%. Because of the low condensation rate in the outer tube, the gas is cooled significantly. The He fraction increases from 4.3% at the top to approximately 22% at the bottom. A net (upward) buoyancy force exists in the tube, since the effect of the increasing He fraction dominates over the temperature effect. The buoyancy force effectively balances the downward pressure force originating from the forced flow through the PCC. Hence, the flow is normal, not reverted.
Case 2B is a transient calculation of 20 s physical time, in which the flow field as calculated in case 2A is used as initial condition. Figure 15 shows the conditions in the PCC tubes at the end of the transient. For the outermost tube, the upward buoyancy force on the He bubble in the lower part of the tube now exceeds the downward pressure force because of the decreased flow rate in comparison with case 2A. The result is reversal of flow. A new, stable flow field develops in the tube. Hence, the tube is effectively blocked for normal gas flow. Helium flows upwards in the tube, becomes diluted with steam-air in the upper drum, and flows back to the lower drum through the other tubes. Thus part of the He is re-circulated in the PCC. Condensation of steam in the lower part of the tube further increases the He fraction and the associated buoyancy force, driving the process. Flow reversal is accompanied by inversion of the vertical temperature profile, as also found experimentally.

Calculations with FLUENT

The PCC behaviour in Test T1.2 was simulated using CFD code FLUENT 4. Due to the long duration of the experiment, only selected periods were simulated. Two cases were calculated: 1) Steady-state before He-injection, 2) Transient calculation after He-injection. The FLUENT model considered only 1/4 of the of the PCC geometry due to symmetry reasons. Standard k-ε model with wall functions was used for turbulence modelling. A simple condensation model developed at VTT was used in the simulation. In the model, the amount of condensation is based on the difference of steam partial pressures at the tube wall and in the flow. The tube wall temperatures and the condensation rate are solved iteratively. Based on the calculated condensation rate, sink terms were defined for pressure, species and enthalpy equations.

The simulation reproduced the flow reversal that was observed in the experiment, but quantitatively the prediction of condensation rate was not correct. In the case 1 of no helium and only residual air in the steam, the condensation rate was underestimated in the calculation by almost 50 %. The temperature profile along one tube in the simulation clearly indicates that the condensation was not complete in the PCC, like it was in the experiment. In case 2 (transient calculation with He-injection) the condensation rate was slightly overestimated. The flow

reversal, as the helium concentration increased in the lower header, occurred also in the simulation (Figure 16). Main reasons for the differences between measured and simulated condensation rates are probably inaccuracies in modelling boundary conditions (PCC pool heat transfer) and turbulence. The detailed results are given in [28.29].

C.2.3 Conclusions on Analytical Investigations

The global system response including distribution of non-condensable gas and steam in the DWs could be captured fairly well by the all the codes applied (GOTHIC, CFX , STAR-CD). The prediction of the PCC behaviour in the presence of light gas turned out to be quite challenging for the CFD codes CFX and FLUENT. The effect of flow reversal that has been observed in the experiments could be qualitatively reproduced by both codes. In summary, the extended experimental database and the improved codes will contribute to a more accurate design basis that will allow for further optimising passive safety features.

C.3 Wetwell Gas Space Modelling and Performance Assessment

Accurate prediction of containment pressure transients during severe accidents requires capabilities for 3D modelling of natural convection, mixing and stratification of multi-component gases, and condensation as well. These modelling capabilities must be reliable, validated and suitable for engineering practice. Therefore, medium-scale tests in the KALI facility have been performed in order to provide an extended database, which is suitable for the validation of CFD models. Also, the KALI tests were aimed to investigate if helium is suitable to substitute hydrogen in PANDA system tests aimed to simulate the response of containment and passive safety systems in the case of a BDBA with release of hydrogen. The KALI separate effect tests provided gas temperature and concentration spatial distribution during transient test in which hydrogen or helium and steam were injected into the vessel.

C.3.1 Separate-Effect Test Programme in KALI

The test facility KALI [30] consists mainly of a pressure vessel of 2.1 m in diameter and 4.6 m in height. Auxiliary systems allow for pre-conditioning the facility to the test initial conditions and to inject and purge gas and/or steam during a test. The maximum operating conditions for pressure/temperature are 12bar/200°C, and up to 10% of dry air for the hydrogen molar concentration. Figure 17 shows a schematic of the facility. The locations for temperature and gas concentration measurements inside the vessel are shown in Figure 18.

Test Specification

In the KALI transient tests hydrogen or helium and steam mixture is injecting in a closed vessel. Before injection starts the vessel walls are preheated to 80°C and the air atmosphere is at 80°C and 2 bar. These conditions represent the status of the wetwell during PANDA tests. The diameter of the injection pipe is 200 mm, based on scaling considerations. The molar fraction of H2 or He and steam mixture injected to the vessel ranges from 100% / 0% to 60% / 40%. The temperature of the injected gas is 140 °C and the flow average velocity ranges from 0.2 m/s to 1 m/s. The injection time is defined to get the expected final average molar gas concentration at the end of injection. The final concentration ranges from 8% for H2 test to 15% for He tests. For comparison of He and H2 tests, similitude rules were applied to select the relevant parameters to get similar test injection conditions. This concerns the average final molar concentration, the injection pipe geometry and the Richardson number at the beginning of the injection. Table I summarizes the main characteristics of the KALI tests [30].

KALI Experimental Results

Concerning initial test conditions, an inhomogeneous temperature distribution in gas space and vessel walls could not be avoid. The reason seems to be heat losses through the vessel wall which are not homogeneous. We can also suppose an effect coming from the natural convection above the pre-heated injection pipe. Despite we were particularly vigilant with the uniformity of these temperatures it was impossible to get a better homogeneous distribution under the conditions initially defined in the test matrix. Thus, the strategy consisted in having as much as possible the same initial temperature distribution for all tests. As a homogeneous distribution could be obtained at room temperature, we performed an additional test at "cold" initial atmosphere, to assess the influence of this initial temperature distribution. Some difficulties to obtain stable injection temperature and velocity were encountered. It could be relevant for codes interpretation that during the injection period the velocity field at the outlet of the injection pipe was not completely homogeneous and depends on the use of the additional porous plate at the outlet of the injection pipe. The results should be considered only like possible trends, since the test conditions are very different and the accuracy of the measurement was not so good. By looking at the global evolution of the concentration and temperature measurements during the injection period, we can consider that the gas mixing is driven by forced convection effects, since a correlation is observed between the injection velocity and the first concentration and temperature measurements located in the central vertical axis of the vessel, above the injection pipe. Important information concerning the injection period is that the gas injected is immediately mixed with the initial air atmosphere. At the end of injection, the gas convection obviously has a slower kinetics, resulting in buoyant convection and diffusion effect. By looking at the concentration measurements we can see a spatial and temporal evolution of the gas stratification. After the injection the concentration distribution of the light gas splits into two distinct areas: a lower concentration rate in the lower middle volume of the vessel and a higher concentration in the higher middle volume. The transition zone between these two volumes moves up along the vertical axis, initially located in the lower level (at about 1.4 m) without over passing the height of 3.4 m. Thus, the light gas seems to concentrate more in the lower part of the vessel, overtime. By comparing the evolution of the measurements located on the central vertical axis and those located on the vertical axis at 0.7 m from the central axis, the variation of the light gas concentration in the transition zone seems to be more precocious and faster in the centre of the vessel than close to the wall. The light gas concentration seems to be homogeneous on each horizontal section. By examining the temperature, we can observe a regular decrease in temperature during the test, mainly driven by the heat losses through the vessel wall. The complementary analysis related to the reproducibility of the KALI test, the axis-symmetrical behaviour in the vessel, the similarity between helium and hydrogen tests and the various separate effects, is based on a comparative approach, consisting in underlining the particularity observed in each test compared to the global behaviour. From these observations, we concluded that reproducibility in KALI is of suitable quality. The detailed KALI results are given in [31].

Similarity between helium and hydrogen tests was investigated by comparing test 1.1grid of 15/10 (He) and test 1.2grid of 28/10 (H2). The injection temperature of hydrogen test is about 15 °C lower than for helium test. The average velocity field in the injection pipe, just upstream of the outlet area, is similar for both tests. The gas mass injected is 11% higher for H2 test than for He test. The global evolution of the concentration after injection, shows that the kinetics of the spatial gas mixing evolution is slightly slower for H2 than for He. This is confirmed by the "instantaneous" concentration and temperature distributions within the vessel for various instants after beginning of injection. This tendency probably comes from the difference in the injection temperature. For the same initial conditions, a lower injection temperature leads to a

slower kinetics of the spatial gas mixing evolution. We can see a difference in the light gas concentration rate, which is higher for H2-test than for He-test by about 1% after the end of injection. In particular, the "instantaneous" concentration and temperature distributions within the vessel for various time after the beginning of the injection allow us to get a clear view on that point. This difference mainly comes from the difference in the gas mass injected. The pressure of the initial air atmosphere, which is lower for the H2 than for the He-test, reinforces the difference. The difference in the measured concentration rate, seems to be consistent with this analysis. By looking at the temperature measurements, we see that the regular decrease all along the recording duration is similar for both tests. From this comparison between H2 and He tests, we consider that the gas mixing and stratification behaviours are close for both tests.

C.3.2 Analytical Investigations

Simulation of Gas Space Mixing with GOTHIC

The validation of GOTHIC mostly refers to the analysis of the two KALI tests without the third grid (porous plate), and makes nearly exclusive use of data on helium or hydrogen concentrations. The conditions investigated are considered of general use for assessing the code capabilities to predict mixing in a single vessel driven by a strongly buoyant plume [32]. The prediction of stratification with GOTHIC can only be done by taking into consideration turbulence. Calculations with the laminar flow model resulted in over-prediction of stratification and substantial delay in the propagation of He in the lower half of the vessel, even when a coarse mesh was used. The standard k-ε turbulence model in GOTHIC tends to predict smaller values of the turbulent diffusivity than predicted by commercial CFD codes, and seems to be adequate to provide upper bounds for the strength of the stratification. This model seems to be sufficient for best-estimate predictions for light gas distribution. The RNG k-ε turbulence model as well as other models that are often taken into consideration as alternative to the expectedly too diffusive standard model, when implemented in GOTHIC seems not to be superior to the standard model. The standard model tends to under-predict mixing, so that a model that further reduces turbulent diffusivity can only find application in sensitivity studies. Concentrations and concentration gradients along the vessel axis (inside plume) were all strongly over-predicted using the reference, fine-mesh model, and the nearly perfect mixing in the upper half of the vessel could not be reproduced. Concentration gradients have also been overestimated in the bulk of the fluid. A very positive result is that the propagation of the gas concentration front in the nearly stagnant region of the flow domain (lower half of vessel outside plume) is predicted fairly well. This is especially remarkable in view of the importance to predict the accumulation of hydrogen in the zones of a multi-compartment containment where little mixing is driven by weak convective currents. A coarse mesh seems to be able at reproducing the results obtained by means of a fine mesh used for most of the 2D calculations carried out. The results obtained (shown in Figure 19) are very important in consideration of the practical applications of GOTHIC for containment analysis, where 3D models are required and only a coarse mesh can be afforded. In principle, it should be verified that the quality of the predictions obtained with a coarse mesh using a 2D model is still adequate when using a 3D model. The results depend on the turbulence level at the injection. As the turbulent viscosity at the outlet of the pipe is under-predicted by GOTHIC (with respect to predictions with a CFD code), mixing is under-predicted using the reference mesh. However, with a different representation of the pipe exit region, which was leading to higher turbulence levels, the code could correctly predict the helium dilution along the axis of the plume. This result is of little practical consequence, as for safety calculations the geometry of the source (break) is not known and assumptions must be made. Moreover, the influence of the injection conditions are somewhat overemphasised in the tests analysed, as the KALI vessel is small and the aspect ratio of the plume is low and not representative of realistic conditions in the containment. In summary, GOTHIC showed its

capability to provide reliable predictions of mixing in a single vessel using the standard k-ε turbulence model, and simulations with a coarse mesh seem to be adequate. Limitations of the code include inaccurate prediction of turbulence close to the injection and lack of a model, which can account for the effect of bulk velocity on the heat transfer rate between fluid and structures. Both limitations, however, are related to the non-prototypical conditions of the KALI tests, and are not expected to have a major significance in safety calculations for NPP containments.

Calculations with CFX-4

KALI experiments relevant to the response of the wetwell during postulated accident were simulated with CFX-4 [33]. The focus of the calculations was on modelling of the transient gas distribution in the vessel, upon He or H2-injection into the initially air-filled vessel. All computations are conducted for the 2D axis-symmetric case. Scooping calculations with GOTHIC had previously suggested that a reverse flow might occur at the pipe outlet in the case of low-velocity injection. Indeed, the performed analysis revealed intermittent intervals of reverse flow in the pipe, occurring in the initial phase of injection. However, the nature of gas in the pipe was further clarified. The results showed that it should be attributed to the turbulent diffusion (instead reverse flow). The calculated pressure shows a good agreement with experimental data (Figure 20). Almost all concentrations are predicted very well with the standard k-ε turbulence model, as shown in Figure 21. Only at the location where the injected gas arrives at latest, the gas front propagation resulted in a moderate over-prediction. The RNG k-ε turbulence model proved to be capable of accurately predicting concentration at this point. In the case with pipe area reduction (by means of perforated plate), acceptable predictions were obtained. Because of uncertainties in the inlet temperature and the initial wall and gas temperatures, as well as probable non-homogenous heat losses, a reliable comparison between the simulated and measured data is difficult. In the tests with the perforated plate, both concentrations and temperatures are controlled by the mixing patterns at the mixing chamber exit. The importance of the accurate resolution of turbulent diffusion downstream the mixing chamber exit, and the mesh effect are emphasised. Inconsistency in some test data does not allow a statement whether He can represent the behaviour of H2. In summary, the results obtained showed that CFX4 is capable of reliable prediction of buoyant flows in the simple confined geometry, if the turbulence is properly accounted for. The predictions are better for higher injection velocities where buoyancy is less dominant.

Calculations with CFX-5

Two KALI experiments T1.1 (15/10) and T1.2 (28/10) were simulated with CFX-5 [34]. The simplicity of the test vessel suggests the creation of a purely structured grid. Although symmetry could be used to save computing resources, it was decided to create a full 3D model and use the simulations as a test for larger and non-symmetric arrangements. It is also known that some mixing effects only develop in a full 3D representation of the experimental setup. Three grids with different resolution above the injection pipe and close to the outer walls were investigated. The number of cells varies between 50496 and 207872. Both selected experiments are identical except the properties of He and H2. The code options used are: Two component mixture (H2 or He in air) and turbulent flow with shear stress transport model with scalable wall functions. Heat losses to the outer walls are considered with a constant heat transfer coefficient. The outflow pattern from the injection pipe is assumed to be purely flat and vertical. This is justified by the additional grid close to the upper end of the pipe, introduced to avoid back flow into the pipe. The gas atmosphere in the vessel is completely calm but has temperature stratification of 6 to 10 °C. The stratification is accordingly applied to the outer walls. From the given gas temperatures, it can also derived that there was not only a vertical but also horizontal

profile. Figure 22 shows for Test T1.1 the distribution of temperature, helium and velocity during the inflow of He close to the end of the injection phase. The pressure history is shown in Figure 23. The comparison made with three sensors in the mixing chamber shows good agreement. The He mole fraction distribution is simulated very well (Figure 24). The test data did not completely describe the temperature distribution by the coarse grid of sensors. Hence, it was not possible to capture all details. Remaining disagreement of the simulations with the measurements may be caused to some degree by the mismatch of test boundary and initial conditions. This makes it difficult to answer the question about the substitution of hydrogen by helium in experiments. Furthermore it is hard to evaluate the models in CFX in terms of turbulence, mixing and heat transfer. For the He experiment T1.1 a better agreement with the measured data was achieved compared with the H2 test T1.2. On the computational side care was taken to exclude most of possible adverse affects on the quality of results. Therefore several meshes with a high number of cells were created and the vessel was set-up as a 3D model, although symmetry could be used. In the 3D model influences of the code solver on the symmetry of the solution could be studied.

Calculations with STAR-CD

In STARD-CD buoyancy forces are taken into account. Other physical properties (specific heat, viscosity, thermal conductivity) are mass weighted averages. The mass fraction of each species is solved via transport-diffusion equation. For turbulence modelling a standard number k- ε model has been used. For the grid a 2D axis-symmetric model is used. The wall temperatures are not uniform. The air is hotter at the vessel top and colder near the wall. For all tests, despite the use of grids we have a 3D distribution of the velocity field at injector outlet. The gas is mainly injected in one side of the injector. This is probably due to the anti-detonation system, upstream the injector. We must distinguish the temperature of the gas at the outlet of the injector and the gas temperature far upstream the injector. For all tests, the gas at the outlet of the injector is colder than those upstream despite the thermal insulation and the specific electrical heaters. The temperature difference is nearly 50 °C, excepted for the test T6bis, where it is nearly 10 °C. We think, that at the outlet of the injector we have lot of turbulence. Consequently, the injected hot helium (or H2) is quickly mixed and cooled by the surrounding cold air initially in the vessel. These mixing and cooling effects are less efficient when the injection velocity is high. This is the case in test T6bis. As we do not consider any grids in our calculations, we have not only considered that pure and hot He (or H2) is injected in the vessel. We have also considered a mixture [He (H2)+air] with a given temperature. STAR-CD results are reported in [35]. We used the He test T1.1 of 01/08. The conditions in the initially are 2 bar and 75.5 °C and the injection temperature is 85 °C. Two kinds of calculations with an injection of 100 % He with adiabatic condition and with an injection of a mixture with 38.7 % He with wall heat losses were considered. Injected He leads to very high concentration values. To have better results, we have chosen to inject a mixture with 38.7 % helium. We can see that the code is able to reproduce the measured concentration time history. It became clear that we need to consider heat losses at the wall. The velocity fields calculated for two different transient times are shown in Figure 25.

C.3.3 Conclusions on Code Performances

Based on the 2D studies carried out, the GOTHIC code is capable to provide reliable predictions of mixing in a single vessel using the standard k-ε turbulence model, and simulations with a coarse mesh seem to be adequate. In the future, the assessment should be focussed on multi-compartment geometries, using 3D models. Limitations of the code include inaccurate prediction of turbulence close to the injection and lack of a model which can account for the effect of bulk velocity on the heat transfer rate between fluid and structures. Both

limitations, however, are related to the non-prototypical conditions of the separate-effect tests in KALI, and are not expected to have a major significance in safety calculations for containments. The results obtained with CFX-4 lead to the conclusion that the code is capable of reliable prediction of buoyant flows in a simple confined geometry, if the turbulence is properly accounted for. These predictions are better for higher injection velocities where buoyancy is less dominant. The experiments were analysed with CFX-5. Because the test data are quite non-uniform, and concerning the gas temperatures not completely described by the coarse grid of sensors, it was not possible to capture all details in the simulations. For the He-test a better agreement with the data was achieved compared with the H2-test. The STAR-CD study concerns the results from He-test T1.1. The code demonstrated its capability to reproduce the concentration time history.

C.4 Plant Evaluation

TEMPEST was devoted to study passive decay heat removal systems for advanced BWRs, in particular the ESBWR and SWR1000. The results reported in the previous chapters were translated to the plant level. Plant analyses of the SWR1000 were performed with the codes SPECTRA and WAVCO. Improved models and insights obtained from PANDA BC4 test, new PANDA and KALI tests on the effect of stratification on containment end pressure were applied. Concerning SWR1000, one severe accident scenario was analysed in order to demonstrate the simulation capability of the validated models. Concerning ESBWR, the impact of the project results on potential containment simplification and plant safety are assessed.

C.4.1 SWR1000 Containment Analyses

For the SWR1000, a core melt scenario after a stuck open safety valve accident was selected for analysis. Full-scale calculations of the complete multi-compartment containment with a complete Building Condenser design were performed with the LP codes SPECTRA and WAVCO. The analyses served first, to obtain an estimate of code-to-code differences on results of plant analyses. This was to be achieved through a comparative analysis of a common accident scenario for the SWR1000 with SPECTRA and WAVCO. Second, to estimate the effect of gas space stratification modelling on the predicted containment end-pressure. This was to be achieved through a sensitivity study with SPECTRA. Third, the functioning of the BC in the presence of hydrogen was evaluated. The passive decay heat removal system for SWR1000 (Figure 26) consists, among others, of the BC, a tube heat exchanger placed near the top of the DW. Experimental investigation of the BC performance has been performed in the PANDA facility. Test BC4 has been designed to study the BC performance under severe accident conditions, with hydrogen being generated in the core, and released to the containment. This test has been analysed using both CFD [10] and system [11] codes. It was concluded that with CFD codes one can predict accurately gas stratification in certain parts of the containment, and that this stratification leads to lower containment pressure than calculated by a system code with perfectly mixed control volumes. A real size SWR1000 power plant was investigated. The computer model of SWR1000 was built for SPECTRA and WAVCO. SPECTRA contains models allowing the user to force stratification in certain parts of the system. The Parametric Density Stratification model was used in several sensitivity calculations to investigate the influence of stratification on the containment pressure in the full size SWR1000 plant. The same accident scenario for SWR1000 was analysed by WAVCO and SPECTRA. Comparison of results obtained with the two codes allows to estimate the uncertainties related to differences in code models as well as the user effect, such as choice of nodalisation, optional models, etc.

WAVCO Calculations

According to LP code practice the SWR1000 containment was modelled as a system of nodes (35 zones, 78 connections). Another 34 nodes with 36 connections were used to model the BCs with associated piping and the Shielding/Storage Pool. The compartments with BC were represented using four nodes. This nodalisation promotes stratification and therefore the WAVCO analysis is expected to give conservative results concerning the containment pressure. In the SPECTRA model each compartment was represented by a single volume, but in SPECTRA analysis gas density stratification was imposed on these volumes. Therefore, SPECTRA and WAVCO give conservative pressure estimation. The BC pool was divided vertically in four nodes. This nodalisation results in strong thermal stratification, as only the upper node is heated by the hot water from the BC outlet and no mixing with lower nodes is allowed by using a single stack of computational cells. This is a good representation of the reality, although not conservative because BCs are always supplied with the coldest water available, making their cooling capacity most efficient. Stratification of the BC pool has very little influence on the overall results. The WAVCO results [36] are summarized as follows: Non-condensable gases are transferred from the DW into the WW only during two restricted time intervals of the whole event sequence: In the initial phase when most of the original nitrogen contents is pushed and flushed out of the DW, and in the third phase when part of the released H2 is pushed into the WW. In both cases only the narrow H2 vent pipes are sufficient to maintain the pressure difference between DW and WW below the clearing pressure of the large vent pipes. The strong temperature stratification in the flooding pool ensures that the BCs are always supplied with the coldest water available, making their cooling capacity most efficient. These heat removal powers, derived from the BC's inlet and outlet water temperatures and the mass flow rates, are shown in Figure 27. From this diagram the positive effect of a high steam concentration as well as the negative effect of a high hydrogen concentration upon the Building Condenser performance is obvious. Depending upon the operation conditions the cooling power of one BC varies between ~0.2 MW (dry atmosphere) and ~4 MW (superheated steam with low gas admixture). The maximum containment pressure of the discussed accident sequence amounts to 4.7 bar and is reached during the release of very hot steam and hydrogen after core dump (Figure 28). To the end of the calculation the pressure has fallen to 3.6 bar.

SPECTRA Calculations

The SWR1000 accident scenario analysed with WAVCO was also analysed with SPECTRA [37]: First, to determine the sensitivity of the calculated results, in particular the prediction for containment end-pressure, to possible stratification in containment volumes. Second, to provide a code-to-code comparison with WAVCO. Comparison of results obtained with two different codes allows to estimate the uncertainties related to differences in code models as well as the user effect, such as choice of nodalisation, optional models, etc., but does not allow statements on code accuracy, because of the absence of experimental data.

The model used for sensitivity studies was somewhat different from that used for the code-to-code comparison. The sensitivity runs were performed with a stand-alone SPECTRA model of SWR1000, while the SPECTRA/WAVCO comparison was performed using the source from the primary system as calculated by MELCOR. The primary system results obtained from MELCOR and SPECTRA were very similar. Three sensitivity cases were analysed in order to investigate the influence of hydrogen stratification on the calculated containment pressure:

1. Run SOSV. Perfect mixing case: typically analyses with system codes are performed using the perfect mixing assumption.

2. Run SOSV-S. Stratification in the CF pool volumes (gas space around the BC units).
3. Run SOSV-SP. Stratification in the Passage Rooms (volumes without BC).

When stratification was active, H2 was assumed to create an almost perfectly stratified layer at the top of a given Control Volume. In the stratified case SOSV-S the high H2 concentration around the BCs degraded their performance and caused the containment pressure to increase more than in case of well mixed volumes. At the end of the analysed period, the H2 level stabilised at about middle elevation of the BCs. The H2 level increases until condensation on the "uncovered" part of the BC units approximately balances the steam produced in the core. At such time the pressure stops increasing, and the system becomes approximately stable. In the well-mixed case (SOSV) H2 is distributed evenly, however the self-stabilising property of the system, discussed above, still works. This time the pressure stabilises when the hydrogen is diluted to such a degree that the condensation on the BC units approximately matches the steam production in the RPV. Finally, in the run SOSV-SP Hydrogen creates a stratified layer in the Passage rooms between the Building Condenser compartments. This allows trapping more H2 in these rooms and preventing it from being vented into the Suppression Pool. Consequently the final containment pressure is lower.

The CFD analyses of PANDA BC4 test have shown that strong stratification developed in the volume without BC. Simultaneously the volume around BC remained well mixed; a consequence of a strong jet of incoming gas. In case of the SWR1000 plant the gas from the primary system enters the containment in the compartments containing BC. Therefore it is expected that the case (c) in Table II is the most realistic case. It is concluded that results obtained with well mixed volumes (typical system codes) are expected to give conservative containment pressure. In the analysed scenario the overestimation of the pressure by a "well-mixed" code is about 7%. This conclusion will not be valid in case of a scenario in which stratification would develop in the volume around the BC units. In such case the results obtained with the well-mixed volumes would be too optimistic. The results shown in Table II indicate that the underestimation of the pressure would be about 6%. The question whether stratification would or would not develop in certain parts of the system can only be answered by detailed CFD analyses involving the critical parts of the containment. It is therefore recommended that in the analyses of SWR1000 and other advanced plants, CFD calculations should be performed as supplementary calculations, to determine whether stratification might be expected and where. To limit the computational expense, the CFD computational domain should be limited to the critical parts of the containment; the necessary boundary conditions at the cut-off points would be taken from a system code. If no CFD analysis is performed, then a bounding case should be sought using sensitivity study.

SPECTRA/WAVCO Comparison

The SPECTRA/WAVCO comparison is discussed in [36]. The scenario analysed by SPECTRA [38] and by WAVCO was somewhat different from the scenario analysed for the sensitivity study. The main difference was the uncovered safety valve outlet. As a consequence, very hot steam (above 1100 K) coming from the reactor vessel at about 28,000 s was entering the space around the BC units directly, without first passing through the pool. The gas temperatures around the BC pool exhibit a sharp peak around this time. The same is happening with the BC power and the containment pressure. The containment pressure reached its maximum value during the relatively short peak around 28,000 s. The peak pressure was equal to 5.4 bar in SPECTRA and about 4.7 bar in WAVCO. The code-to-code discrepancy is therefore equal to about 13%. It should be noted that the SPECTRA run was made with stratification maximised around the BC units. Using the numbers in Table II one can estimate that in case of perfect mixing in those volumes, the SPECTRA peak pressure would be 0.3 bar

lower, which means 5.1 bar. The code-to-code discrepancy would in such case be about 8 %. In WAVCO the space around the BC units was divided into several control volumes. With this division hydrogen stratification has developed, as well as gas temperature stratification with hot steam residing in the lower part of the compartment and cold hydrogen in the upper part of the compartment. This is evidently different from SPECTRA where this inverse temperature stratification could not be calculated by definition, since the compartments were represented by single control volumes. The significant stratification calculated by WAVCO is a consequence of the nodalisation chosen for the compartments around the BCs. The hydrogen and hot steam enter the lower part of the compartment and condensation occurs in on the BC surface. The applied nodalisation does not promote natural circulation, and therefore a relatively large stratification is obtained. (This will be the case with all system codes, and is not WAVCO specific). If an alternative nodalisation is applied, one that will allow natural circulation, mixing will be mach better and the degree of stratification smaller. The fact that the results will depend strongly on the applied nodalisation makes it impossible to use typical system codes, such as WAVCO, SPECTRA, as well as RELAP, TRAC, etc., to predict stratification. For that CFD codes are necessary. Moreover, presence of stratification depends on factors such as jet formation at the source from the primary system. The reason for obtaining well-mixed condition in the volume around the BC unit in test BC4 was a jet of gas coming from the RPV. In general, stratification may develop when energy of incoming fluid is low (plume formation) while it cannot develop when the energy is large (jet formation). The phenomena involved are quite complicated, and difficult for numerical simulation. They can be successfully simulated only using a CFD code with an advanced turbulence model.

C.4.2 Impact of TEMPEST Results on SWR1000 and on ESBWR Design

The BC operation is characterised by a self-stabilising property; the pressure stabilises when the non-condensable gases are diluted (purged to the WW) to such a degree that the condensing power matches the steam production in the core. Eventual inaccuracies in the code model of the condensing unit result in additional containment pressure changes needed to stabilise the operation at the same power.

To understand the usefulness of PANDA tests it is necessary to know some key aspects about the ESBWR containment behaviour. A brief description of the system response under conditions relevant to the PANDA tests is provided to understand the relevance of these tests to further develop the ESBWR design. During normal operation the ESBWR containment is inerted with Nitrogen. During a LOCA steam is released to the DW from the RPV forcing a mixture of steam and non-condensable gas into the WW through the PCC and main vents. Compressing gas into the WW is the primary cause of containment pressure increase. During normal operation DW and WW pressure are approximately equal. During an accident the non-condensable gas is swept into the WW and the containment pressure increases. The maximum achievable pressure is obtained when all of the Nitrogen has been swept into the WW. In addition to this, steam entering the suppression pool is condensed and increases the pool temperature. As the surface of the pool heats up, the steam pressure in the WW gas space increases too, contributing to an increase in containment pressure. In the long-term, it is important for the PCC to condense the steam generated by decay heat so that the suppression pool does not continue to heat up and pressurize the containment. The containment pressure is primarily determined by the quantity of non-condensable gas that is in the WW and the amount of energy deposited in the upper layer of the suppression pool. During a severe accident it is possible that the zirconium in the core will oxidize producing hydrogen. This additional gas can also be swept into the WW resulting in increased pressures. Figure 29 shows the range of containment pressures for the amount of hydrogen that would be generated if 100% of the

cladding in the core oxidized during accident. The PANDA tests were run to simulate the conditions with both hydrogen and nitrogen present in the containment.

PCC Behaviour: During the early part of an accident, when the decay heat exceeds the capacity of the PCC, a mixture of steam and non-condensable gas flows through the PCC and to the suppression pool. The PCC condenses steam out of this flow at its maximum capability. There is no accumulation of non-condensable gas in the PCC under these conditions. The heat removal capability of the PCC is reduced in the presence of non-condensable gas. This is shown in Figure 30. Early in an accident, the non-condensable fraction in the DW is high and the degradation of the PCC heat removal is larger. As the non-condensable gas is moved to the WW and the concentration in the DW decreases the degradation decreases too. Later in an accident with decreasing decay heat level the PCC has excess heat removal capacity. Testing and analyses have shown that under these conditions, the PCC self regulates by accumulating non-condensable gas, thereby blanketing parts of the tubes and reducing the heat transfer area. As the decay heat is gradually reduced the PCC adjusts by accumulating more non-condensable gas until the heat removal capacity matches the heat load.

DGRS Operation: The Drywell Gas Re-circulation System (DGRS) reduces the containment pressure by shifting non-condensable gas from the WW to the DW and then keeping the gas in the DW. Figure 29 illustrates that this effect will decrease the containment pressure. The DGRS fan clears stored non-condensable gas out of the PCC and blows it into the DW. The system reaches equilibrium (PCC heat removal matches decay heat load) with a higher concentration of non-condensable gas in the DW. Depending on the size of the fan it is possible that equilibrium will be reached with some accumulated non-condensable gas remaining in the PCC If the DGRS is shut off the containment state will revert to approximately the state it had before the DGRS was put into action: there is no significant cumulative effect from operating the DGRS. This simplified description assumes that the non-condensable gas in the DW is uniformly distributed so that the non-condensable gas fraction at the PCC inlet is the same as it is in the entire DW. As demonstrated by the PANDA tests it is possible for stratification to occur in the DW. This can increase or decrease the impact of the DGRS, depending on the configuration of the stratification.

Implications of PANDA Tests: The primary information gained from the PANDA tests is the proof of principle for the DGRS. The test showed that containment pressure is reduced with the DGRS in operation for both Nitrogen conditions and mixtures of Nitrogen and Helium. The tests also showed that after the DGRS stopped working the conditions rapidly returned to the conditions existing before the DGRS was operated. This means that the DGRS and its power supply would have to be very reliable in order to rely on it for controlling pressure. In addition the test showed that the DGRS was susceptible to degradation by stratification in the DW. The beneficial impact of the DGRS was significantly less than predicted with uniform mixing assumption due to stratification. Although this effect could be mitigated by careful design of the DGRS inlet and discharge locations it pointed to a vulnerability of the DGRS system. In the end, a decision was made to not use the DGRS as part of the base design. The PANDA tests also provided information on containment performance over a wide range of conditions representing the conditions that might be present after a severe accident. The stratification that was induced in the DW and the difficulty in predicting the stratification with numerous computer codes influenced the decision to use a bounding approach for treating stratification for design basis analysis.

C.4.3 Conclusions and Recommendations

From the SPECTRA sensitivity runs it was concluded that the BC operation is characterised by a self-stabilising property; the pressure stabilises when the non-condensable gases are diluted (by pushing them to the WW) to such a degree that the condensing power matches the steam production in the core. Eventual inaccuracies in code model of the condensing unit result in additional containment pressure changes needed to stabilise the operation at the same power. It is further concluded that results obtained with well mixed volumes (typical system codes) are expected to give conservative containment pressure. In the analysed scenario the overestimation of the pressure by a well-mixed code is 7 %. The above conclusion will not be valid in case of a scenario in which stratification would develop in the volume around the BC units. In such case the results obtained with the well-mixed volumes would be too optimistic. Results indicate that in the analysed scenario the underestimation of the pressure would be about 6 %. From code-to-code comparisons it was concluded that the discrepancy in containment pressure of about 8 – 13 % is attributed to code-to-code differences. Typical system codes, such as WAVCO, SPECTRA, RELAP, TRAC, etc., are not suitable to predict stratification. Stratification may develop when energy of incoming fluid is low (plume formation) while it cannot develop when the energy is large (jet formation). The phenomena involved are quite complicated, and difficult for numerical simulation. They can successfully be simulated only using a CFD code with an advanced turbulence model. For plant modelling it is recommended that in the analyses of SWR1000 and other advanced plants, CFD calculations should be performed as supplementary calculations, to determine whether stratification might be expected and where. To limit the computational expense, the CFD computational domain should be limited to the critical parts of the containment; the necessary boundary conditions at the cut-off points would be taken from a system code. If no CFD analysis is performed, then a bounding case should be sought, using a sensitivity study.

D. CONCLUSIONS AND RECOMMENDATIONS

The cooperation between the seven project partners from five different countries has turned out to be beneficial for the project and as such a relevant contribution to the overall objectives of the 5th Euratom Framework Programme in the area of "Evolutionary Safety Concepts" has been accomplished. The experimental as well as the analytical work were of high quality. The impact of hydrogen on passive safety systems and on containment pressure has been studied. The new experimental data represent a significant addition to the database and, because of their improved spatial resolution they are especially suited for the validation of CFD codes and other codes with 3D capabilities. CFD codes were shown to be able to accurately predict stratification in gas spaces and water pools. Lumped parameter codes showed overall satisfactory performance in passive containment analyses, but tend to over predict system pressure due to their inability to account for stratification effects. Combined LP code and CFD code approaches has been considered for improved performance. TEMPEST substantially contributed to create innovative and validated tools and methods that help to maintain and further improve the safety of existing as well as future reactors. There was not always a consensus between all partners. This is reflected by sometimes different, or even contra dictionary statements related to certain issues addressed in TEMPEST. The main conclusions and recommendations are summarized below:

Validation of Building Condenser System Models: A number of simulations of the PANDA Test BC4 were carried out with various CFD and LP codes (CFX, STAR-CD, GASFLOW, COCOSYS, WAVCO, SPECTRA). Also combinations of CFD and LP codes have been used. The experiment BC4 simulates the system behaviour of the SWR1000

containment with a building condenser, starting during the blow-down phase, for the case of a small leak in the upper part of the reactor pressure vessel and non-operation of the core flooding system. Based on the BC4 calculations, it was concluded that currently only LP codes appear to be able to provide comprehensive predictions for a complex, long time experiment like BC4. Due to limitations in the modeled physics and available computer resources, CFD codes are either restricted to simulate selected periods in time or to include only parts of the problem. CFD codes were also used to support LP codes (combination of CFX – SPECTRA) in understanding special situations or to provide additional information in particular for phenomena related to momentum exchange. LP codes have limitations whenever flow dominates the processes under investigation. The use of CFD enabled an LP code to improve the modelling of mixing in order to obtain more realistic predictions. This resolves a long lasting discussion in which the cause of the consistent over-prediction of LP codes of the containment pressure in PANDA BC tests was attributed to deficiencies of the tests. As was now demonstrated by means of CFD, the discrepancy was due to stratification in the BC stand-by volumes, which was not correctly represented in the LP models. The integral experiments conducted in PANDA have proved to be a challenge to simulation by computer codes. In view of up-scaling to full size geometries found in a containment, code application and development should take into consideration the following: CFD codes will become able to simulate also long-term processes (with increasing computer power and/or parallelization and fast running, robust solver algorithms). The complexity of the physics calls for the implementation of additional models in CFD codes as a standard feature (wall condensation, simplified heat conduction). Also for LP codes is applicable, that models for specific phenomena may be missing. LP codes have clear limitations with processes, which involve momentum dominated transport. Here, the use of CFD codes is advantageous. A recommended trend could be to use LP models to get an overview of a scenario and to conduct parametric studies. CFD codes can be applied for specific and more detailed investigations, identified by previous LP runs. Alternatively, coupled approaches of LP and CFD to split computational regions or to improve the depth of modeling could be applied.

Passive Safety Features Assessment and Optimisation: The performance of the Passive Containment Cooling System (PCCS) of the ESBWR has been experimentally investigated in PANDA for different accident scenarios including release of large amount of hydrogen. (In PANDA H2 was simulated by He). The impact of light gas and its distribution within different containment compartments on PCCS and containment behaviour has been demonstrated. Although, during the He-injection phase the PCCS heat removal capability was degraded, no significant energy deposition in the suppression pool occurred. Shortly after release of helium to the DW stopped the PCCS recovered and the containment pressure finally stabilized at higher level. The pressure increase in an accident with release of light gas is mainly driven by the amount of gas released from the reactor core and less by the degradation of the heat removal capability of the PCCS. The new accident mitigating Drywell Gas Re-circulation System (DGRS) showed its capability to retain non-condensable gases in the DW, thereby slightly reducing containment pressure. In case the DGRS fails, however, the containment pressure will rise within short time to its normal value that would result without DGRS. The steam/helium stratification patterns measured in the DW under very different conditions could be well reproduced by CFD codes (CFX, STAR-CD) and by the 3D code GOTHIC. Calculations with CFX and FLUENT could qualitatively confirm the complex flow pattern indicated by the measurements inside the Passive Containment Coolers (PCC). In summary, the extended experimental database and the improved codes will contribute to a more accurate design basis that will allow for further optimisation of passive safety features with respect to enhanced safety and reduced costs. The behaviour of the PCCs in the presence of non-condensable gas is different depending if the gas is heavier (air, nitrogen) or lighter (H2, He) than steam. Heavier

gases are collected in the bottom region of the condenser. The behaviour of light gas is more complex. When steam is condensing in the tubes, the non-condensable concentration increases, and the density of the mixture decreases. If the concentration of the light gas is high enough, the buoyancy force can overcome the driving pressure difference, and the gas can start to flow upwards in some of the tubes. To better understand the complex flow pattern indicated by the performed PANDA test, new tests with upgraded instrumentation could provide a more detailed insight. Because the PCC units used in PANDA represent just a slice of the ESBWR full-scale unit, scale-up to plant size could also be an issue asking for further clarification. The global system response including the distribution of non-condensable gas and steam in the drywells could be captured fairly well by the all the codes applied (GOTHIC, CFX, STAR-CD). The prediction of the PCC behaviour in the presence of light gas turned out to be quite challenging for the two codes applied (CFX, FLUENT). The effect of flow reversal that has been observed in the experiments could be qualitatively reproduced by the codes. In summary, the extended experimental database and the improved codes will contribute to a more accurate design basis that will allow for further optimising passive safety features with respect to enhanced safety and reduced costs.

Wetwell Gas Space Modelling and Performance Assessment: A series of medium-scale tests has been performed in the upgraded KALI facility to provide an extended database concerning gas mixing and stratification in gas spaces. These separate effect tests provided gas temperature and concentration spatial distribution during transients in which hydrogen or helium and steam mixtures are injected into a closed vessel. The test conditions were close to the WW parameters used in the PANDA tests. One major objective was to investigate if helium is suitable to substitute hydrogen in order to simulate hydrogen effects (as has been done in the PANDA integral system tests). A comparison between a hydrogen test and a helium test, performed in the KALI facility, showed that the gas mixing and stratification behaviours are close for both tests. But, to provide a stronger and more reliable statement, it seems necessary to compare the hydrogen and helium behaviour under additional and various test conditions. The gas stratification and mixing patterns measured in the KALI vessel under different test conditions has been calculated by two CFD codes (CFX, STAR-CD) and also by the 3D code GOTHIC. The calculations could qualitatively confirm the complex flow pattern encountered in the KALI experiments. In summary, these experiments contributed to a better understanding of mixing and stratification phenomena and the extended database allowed for further validating codes for predicting more accurately the gas distribution inside containment compartments.

Plant Evaluation: Pant analysis of the SWR1000 was performed with the SPECTRA and WAVCO codes. Improved models and insights obtained on the effect of stratification on containment end pressure obtained from PANDA BC4 tests, new PANDA and KALI tests, were applied. Concerning the SWR-1000, one severe accident scenario relevant for assessing the BC was analysed in order to demonstrate the simulation capability of the validated models. Concerning the ESBWR, the impact of the results of this project on potential containment simplification and plant safety was assessed. The main conclusions from SPECTRA sensitivity runs were as follows: The BC operation is characterised by a self-stabilising property; the pressure stabilises when the non-condensable gases are diluted (by pushing them to the Suppression Pool) to such a degree that the condensing power matches the steam production in the core. Eventual inaccuracies in code model of the condensing unit result in additional containment pressure changes needed to stabilise the operation at the same power. It is further concluded that results obtained with well mixed volumes (typical system codes) are expected to give conservative containment pressure. In the analysed scenario the overestimation of the pressure by a well-mixed code is 7%. The above conclusion will not be valid in case of a scenario in which stratification would develop in the volume around the BC units. In such case

the results obtained with the well-mixed volumes would be too optimistic. Results indicate that in the analysed scenario the underestimation of the pressure would be about 6%. From code-to-code comparisons it was concluded that the discrepancy in the containment pressure of about 8-13% is attributed to code-to-code differences. Typical system codes, such as WAVCO, SPECTRA, as well as RELAP, TRAC, etc., are not suitable to predict stratification. Stratification may develop when energy of incoming fluid is low (plume formation) while it cannot develop when the energy is large (jet formation). The phenomena involved are quite complicated, and difficult for numerical simulation. They can successfully simulated only using a CFD code with an advanced turbulence model. For plant modelling it is recommended that in the analyses of SWR1000 and ESBWR or other advanced plants, CFD calculations should be performed as supplementary calculations, to determine whether stratification might be expected and where. To limit the computational expense, the CFD computational domain should be limited to the critical parts of the containment; the necessary boundary conditions at the cut-off points would be taken from a system code. If no CFD analysis is performed, then a bounding case should be sought, using a sensitivity study.

References

[1] "Testing and Enhanced Modelling of Passive Evolutionary Systems Technology for Containment Cooling - TEMPEST", Final Report, EVOL-TEMPEST-D15, 2004.

[2] Brettschuh, W., Wagner, K., "Germany`s Next Generation of Boiling Water Reactors", Kerntechnik 61 (1996) 5-6, 1996.

[3] Rao, A.S., Gonzalez, A., "ESBWR – Using Passive Features for Improved Performance and Economics", European Nuclear Conference, Nice, France, 1998.

[4] Dreier, J., Aubert, C., Huggenberger, M., Strassberger, H.J., Meseth, J., Yadigaroglu, G., "The PANDA Tests for SWR1000 Passive Containment Cooling System", 7th Int. Conf. on Nuclear Engineering (ICONE-7316), Tokyo, Japan, 1999.

[5] Hüttermann, B., Heitsch, M., Schwinges, B., "Analysis of Large Pools (Containment Cooler), (COCOSYS/CFX Analysis of the PANDA Building Condenser Exp. BC4 with Large Extended Pools)", GRS-A-2746, 1999.

[6] Hüttermann, B., "CFX/COCOSYS Building Condenser Simulations Part 1: Analysis of PANDA Test BC3 with COCOSYS", EVOL-TEMPEST-D2a-1, 2003.

[7] Klimm, M., "BC4 Simulation with WAVCO", FANP Report NGPS5/2003/en/0112, EVOL-TEMPEST-D2b, 2003.

[8] Starflinger, J., "BC4 Simulation with GASFLOW", EVOL-TEMPEST-D2c, 2003.

[9] Willemsen, S.M., Komen E.M.J., "Modelling SWR-1000 Building Condenser Behaviour, Part A: CFD Validation Analysis of the PANDA BC4 Storage Pool", NRG Report 20407/03.52896/C, EVOL-TEMPEST-D2d, 2003.

[10] Komen, E.M.J., Willemsen, S.M., Roelofs, F., "Modelling SWR-1000 Building Condenser Behaviour, Part B: CFD Analysis of the PANDA BC4 Containment Phenomena", NRG Report 20407/03.53012/C, EVOL-TEMPEST-D2d, 2003.

[11] Stempniewicz, M.M., "SPECTRA Calculations of PANDA BC4 Tests, Calculations Performed within the Combined System Code /CFD Analysis of BC4", NRG Report 20407/03.52376/C, EVOL-TEMPEST-D2d, 2003.

[12] Blanchet, Y., "Validation of CFD Tools: STAR-CD Post-Test Calculations of PANDA BC4 Experiment", CEA Report DTP/STH/LTA/2003-41, EVOL-TEMPEST-D2f, 2003.

[13] Heitsch, M., "Synthesis Report on BC Code Validation, Comparison, Guidelines and Recommendations for Code Use and Improvement", EVOL-TEMPEST-D04, 2004.

[14] Paladino, D., Auban, O., Candreia, P., Huggenberger, M., Strassberger, H.J., "New PANDA Tests to Investigate Effects of Light Gases on Passive Safety Systems", Int.

Congress on Advanced Nuclear Power Plants (ICAPP), Hollywood, Florida, USA, 2002.

[15] Upton, H.A. et al., "SBWR Design Update: Passively Safe Nuclear Power Generation for the Twenty First Century", 4th ASME/JSME Int. Conference on Nuclear Engineering, New Orleans, USA, 1996.

[16] Huggenberger, M., Auban, O., Paladino, D., Candreia, P., Strassberger, H.J., "Hydrogen Impacts on Passive Containment Cooling System and Accident Mitigating Design Features, Part A: Description of PANDA Facility Including Test Specification", PSI Report ALPHA-02-07-0, EVOL-TEMPEST-D06A, 2002.

[17] Paladino, D., Auban, O., Huggenberger, M., Candreia, P., Strassberger, H.J., "Hydrogen Impacts on Passive Containment Cooling System and Accident Mitigating Design Features, Part B: PANDA System Test T1.1, Base Case with Helium", PSI Report ALPHA-02-09-0, EVOL-TEMPEST-D06B, 2003.

[18] Paladino, D., Auban, O., Huggenberger, M., Candreia, P., Strassberger, H.J., "Hydrogen Impacts on Passive Containment Cooling System and Accident Mitigating Design Features, Part C: PANDA System Test T1.2, Stand-by Volume with Helium", PSI Report ALPHA-03-03-0, EVOL-TEMPEST-D06C, 2003.

[19] Paladino, D., Auban, O., Huggenberger, M., Candreia, P., Strassberger, H.J., "Hydrogen Impacts on Passive Containment Cooling System and Accident Mitigating Design Features, Part D: PANDA System Test T1.3, Asymmetric Case with Helium", PSI Report ALPHA-03-04-0, EVOL-TEMPEST-D06D, 2003.

[20] Paladino, D., Auban, O., Huggenberger, M., Candreia, P., Strassberger, H.J., "Hydrogen Impacts on Passive Containment Cooling System and Accident Mitigating Design Features, Part E: PANDA System Test T2.1, Base Case with Helium Injection and DGRS Activated", PSI Report ALPHA-03-02-0, EVOL-TEMPEST-D06E, 2003.

[21] Paladino, D., Auban, O., Huggenberger, M., Candreia, P., Strassberger, H.J., "Hydrogen Impacts on Passive Containment Cooling System and Accident Mitigating Design Features, Part F: PANDA System Test T2.2, Base Case with DGRS, no Helium", PSI Report ALPHA-02-08-0, EVOL-TEMPEST-D06F, 2002.

[22] Auban, O., Paladino, D., Candreia, P., Huggenberger, M., Strassberger, H.J., "Overview of some New PANDA Tests Results: Effects of Light Gases on Passive Safety Systems", Int. Congress on Advanced Nuclear Power Plants (ICAPP), Cordoba, Spain, 2003.

[23] Paladino, D., Auban, O., Huggenberger, M., Andreani, M., "Investigation of Light Gas Effects on Passive Containment Cooling System in ALWR", Int. Topical Meeting on Nuclear Reactor Thermal Hydraulics (NURETH-10), Seoul, Korea, 2003.

[24] Andreani, M., "GOTHIC calculations for representative passive containment cooling system tests", PSI Report ALPHA-04-03, EVOL-TEMPEST-D07, 2004.

[25] Lycklama à Nijeholt, J.A., Komen, E.M.J., "Modelling of the ESBWR Passive Containment Cooling System Performance, CFD Analysis of Condensation and Helium Distribution in the PANDA Drywells", NRG Report 20407/03.53769/C, EVOL-TEMPEST-D8a, 2003.

[26] Blanchet, Y., "Validation of CFD Tools: STAR-CD Simulation of Helium Distribution in PANDA T-series Tests T1.1 and T2.1", EVOL-TEMPEST-D8b, 2003.

[27] Lycklama à Nijeholt, J.A., "Modelling of the ESBWR Passive Containment Cooling System - CFD Analysis of the Effect of Helium on the Performance of the PCCS in PANDA Test T1.2", NRG Report 20407/03.56479/C, EVOL-TEMPEST-D9a, 2003.

[28] Tuomainen, M., "FLUENT Simulation of PCC Behaviour in PANDA Test T1.2", VTT Report PRO1/P7016/03, EVOL-TEMPEST-D09b, 2003.

[29] Tuomainen, M., “FLUENT Simulation of Lighter-than Steam Non-Condensable Gas Behaviour in Vertical-Tube Heat Exchanger”, Int. Congress on Advanced Nuclear Power Plants (ICAPP), Cordoba, Spain, 2003.

[30] Malo, J.Y., Pire, S., ”Experimental Data from the KALI Facility on Gas Mixing and Stratification in a Containment using Hydrogen and Helium Injection, Part A, KALI Experiment Description”, CEA Report DTP/STH/LTA/2003-13, EVOL-TEMPEST-D10A, 2003.

[31] Malo, J.Y., ”Experimental Data from the KALI Facility on Gas Mixing and Stratification in a Containment using Hydrogen and Helium Injection, Part B, KALI Experiment Results”, CEA Report DTP/STH/LTA/2003-42, EVOL-TEMPEST-D10B, 2003.

[32] Andreani, M., “Simulation of Gas Space Mixing using GOTHIC”, PSI Report ALPHA-04-02, EVOL-TEMPEST-D11A, 2004.

[33] Haller, K., “Simulation of Gas Space Mixing using CFX4”, PSI Report ALPHA-04-04, EVOL-TEMPEST-D11B, 2004.

[34] Heitsch, M., “Simulation of Selected KALI Experiments with CFX”, EVOL-TEMPEST-D12A, 2004.

[35] Avakian, G., “Simulation of Gas Space Using STAR-CD (KALI Experiments)”, CEA Report DTP/STH/LTA/2003-36, EVOL-TEMPEST-D12b, 2003.

[36] Klimm, M., “TEMPEST WP4, Calculations of Severe LOCA Accident with SPECTRA and WAVCO using refined models of Building Condenser”, NGPS5/2003/en/0215, 2003.

[37] Stempniewicz, M.M., “Development and Verification of SPECTRA 2.00 Model of SWR-1000”, NRG Report 20407/03.52371/C, EVOL-TEMPEST-D14, 2003.

[38] De Geus, E.A.R., ”Analysis of Safety Valve Opening Accident in SWR1000”, NRG Report 20407/03.52359/C, EVOL-TEMPEST-D14, 2003.

Tables

Table I: Main Characteristics of the KALI Tests

Test	Gas injected	Additional porous plate just at the outlet of the injection pipe (third grid)	Representative temperature just upstream of the outlet area of the injection pipe (°C)	Flow average velocity, calculated from the flow meter measurement (cross section corresponding to Φ200 mm) : [max value obtained during the first seconds of the injection] and stabilized value obtained after the initial peak (m/s)	Injection time	Recording time (from the beginning of the injection)
T1.1 of 01/08	100% He (106 mol)	no	85	[0,7] 0,2	3' 30 s	9800 s
T1.1 of 30/09	100% He (85 mol)	no	95	[1] 0,2	3' 30 s	3800 s
T1.3 of 1/10	100% He (86 mol)	no	115	[0,9] 0,2	3' 30 s	5700 s
T1.1grid of 15/10	**100% He (82 mol)**	**yes**	**145**	**[0,7] 0,2**	**3' 30 s**	**7000 s**
T1.3grid of 27/10	100% He (82 mol)	yes	135	[0,9] 0,2	3' 30 s	10200 s
T1.2grid of 28/10	100% H2 (91 mol)	yes	130	[0,6] 0,2	3' 30 s	8500 s
T6bis of 30/09	100% He (234 mol)	no	125	[1,6] 1	2' 6 s	4700 s
T1.1grid_cold_init_atmos of 29/10	100% He (85 mol)	yes	95	[0,4] 0,2	3' 30 s	9600 s

For all tests : Injection pipe geometry : Φ200mm, initial air atmosphere at 80°C and 2 bar (except test n°1.1grid_cold_initial_atmosphere : about 40°C and 2 bar)

Table II: Influence of Stratification on Predicted Containment Pressure

Case	Containment Pressure at 64,000 s
(a) H_2 stratification around BC units, run SOSV-S	5.0×10^5 Pa
(b) No H_2 stratification, run SOSV	4.7×10^5 Pa
(c) H_2 stratification in passage rooms, run SOSV-SP	4.4×10^5 Pa

Figures

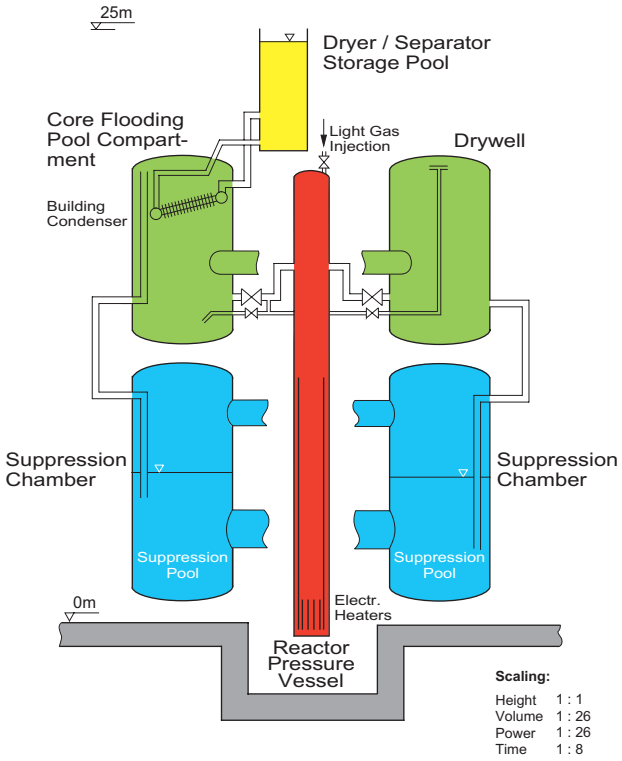

Figure 1: PANDA Facility Configuration used for Integral System Test BC4

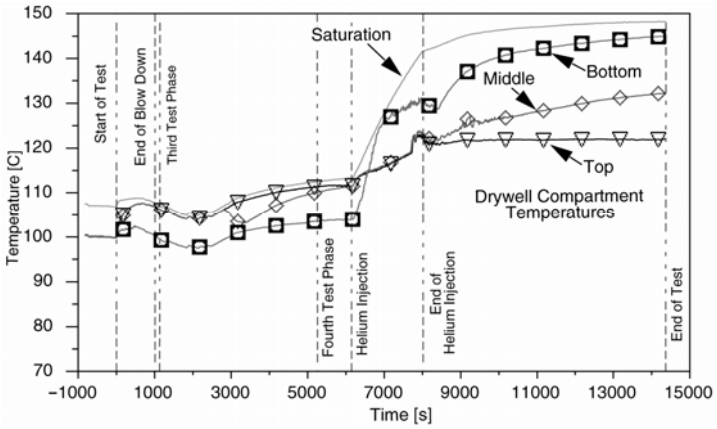

Figure 2: Measured Temperatures in DW1 during different Phases of PANDA Test BC4

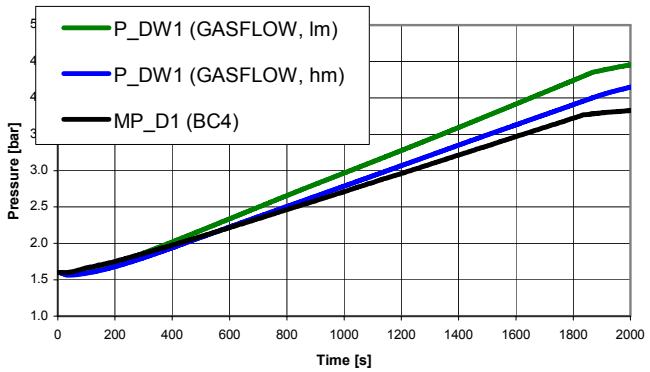

Figure 3: GASFLOW BC Simulations: Calculated and Measured Pressure in DW1

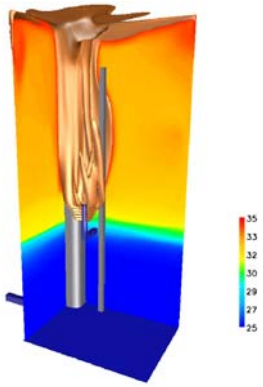

Figure 4: Calculated Velocity Field in the BC Pool

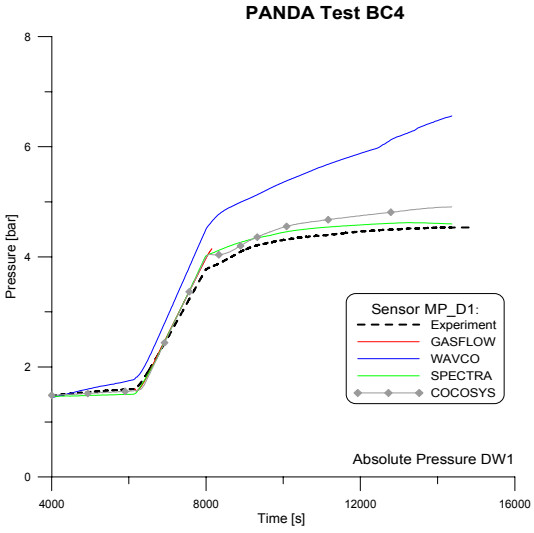

Figure 5: Pressure in DW1; Comparison between Predictions and Experiment

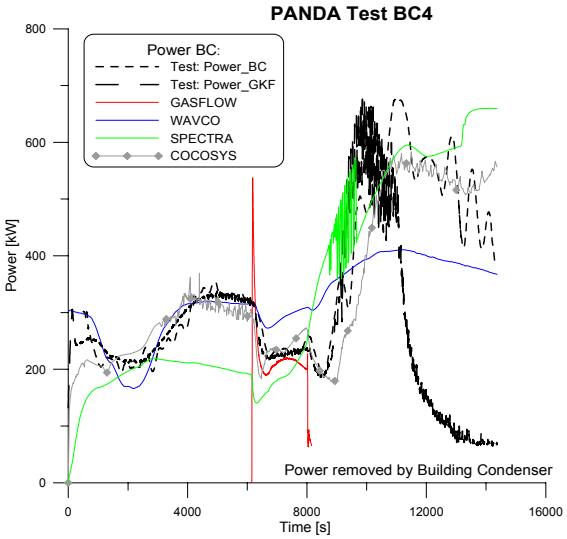

Figure 6: BC Power; Comparison between Code Predictions and Experiment

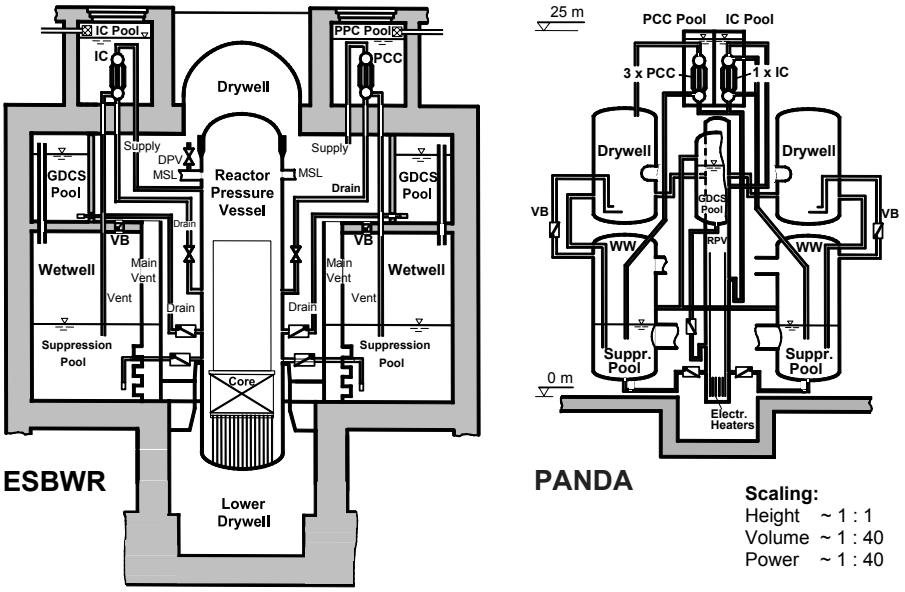

Figure 7: Comparison between ESBWR Containment including Passive Safety Systems and PANDA Facility

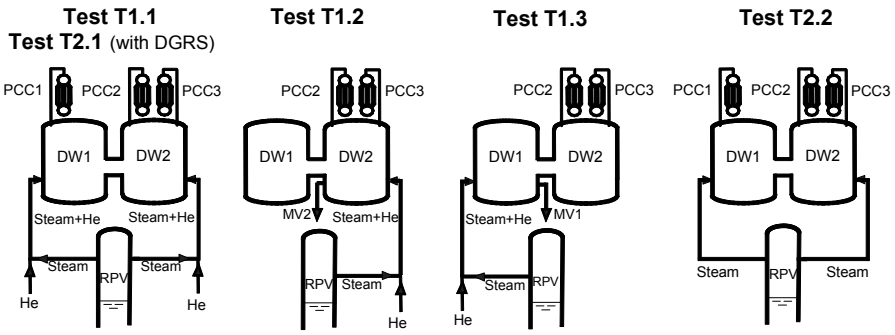

Figure 8: PANDA Facility Configurations for T-series Tests

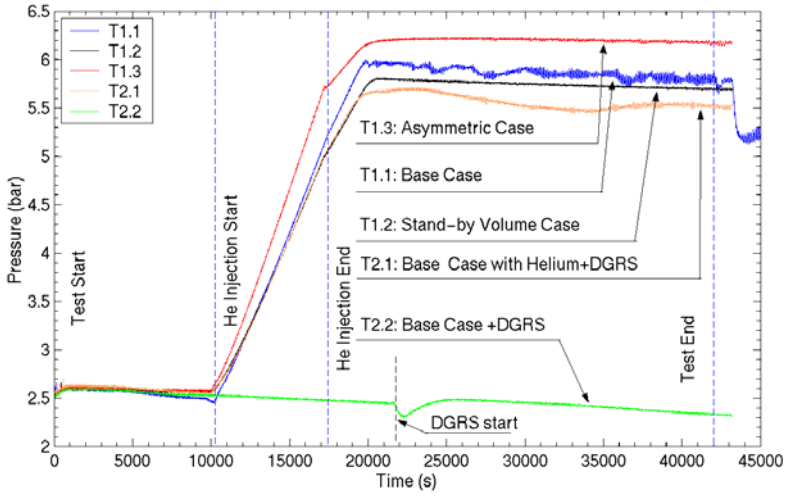

Figure 9: Pressures Measured in the Drywell during PANDA System Tests

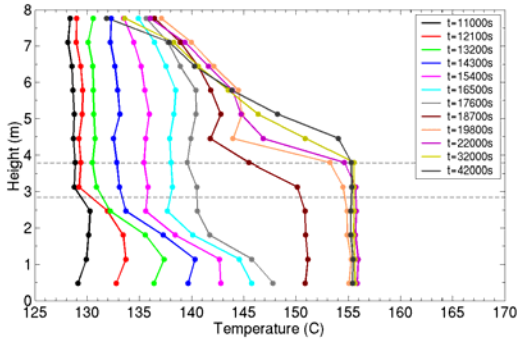

Vertical gas temperature profiles in DW1

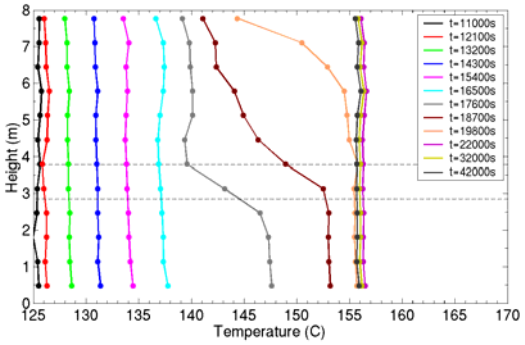

Vertical gas temperature profiles in DW2

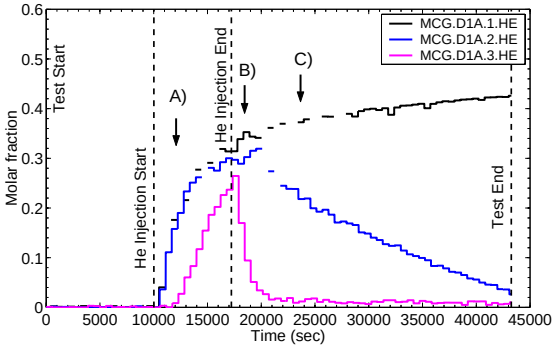

Helium concentrations in DW1

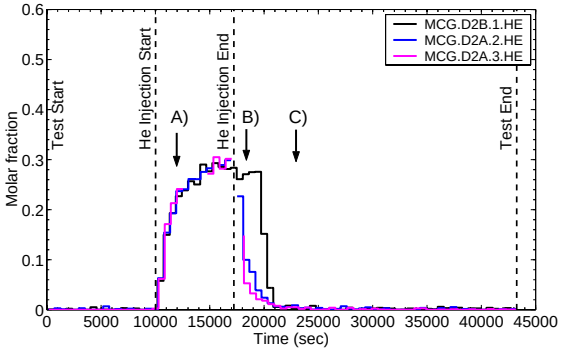

Helium concentrations in DW2

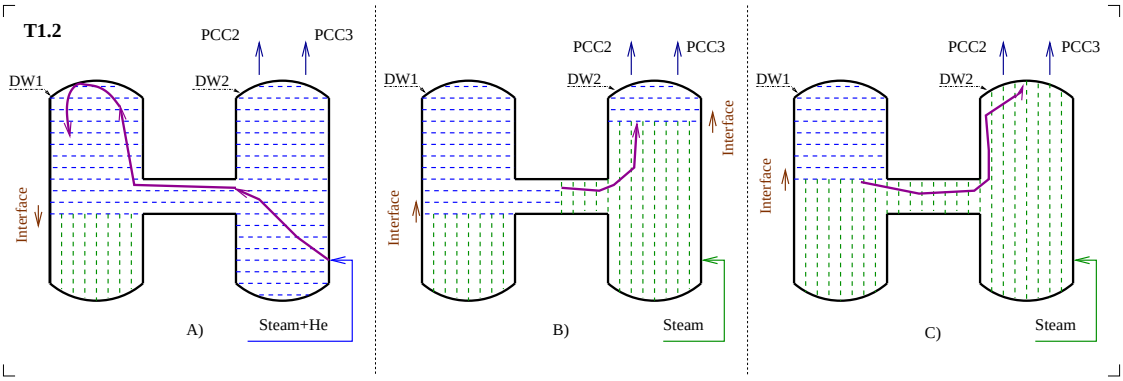

Stratification patterns at transient times **A)**, **B)** and **C)**
(horizontal lines indicate helium-rich mixture, vertical lines indicate nearly pure steam conditions)

Figure 10: Test T1.2: Mixing/Stratification in Drywells; Measured Gas Temperatures (top), Measured Helium Concentrations (middle), Stratification Patterns (bottom)

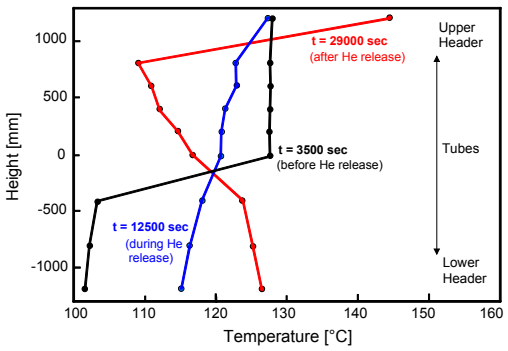

Figure 11: Measured Vertical Gas Temperature Distributions in PCC3 Central Tube and Headers Before, During and After Helium Release (PANDA Test T1.1)

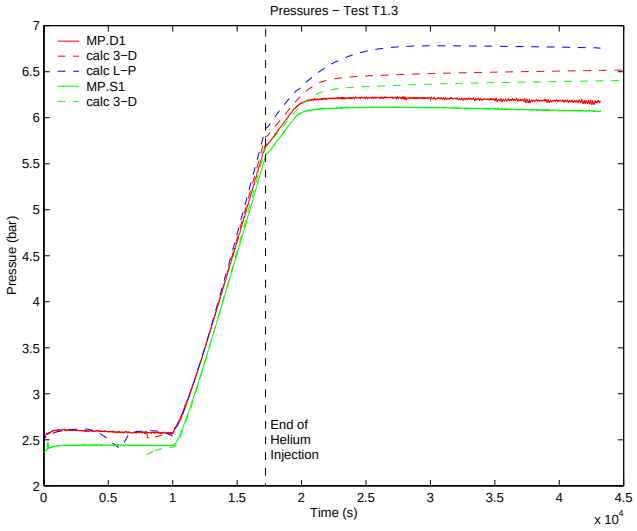

Figure 12: PANDA Test T1.3: Comparison between Calculated and Experimental Pressures

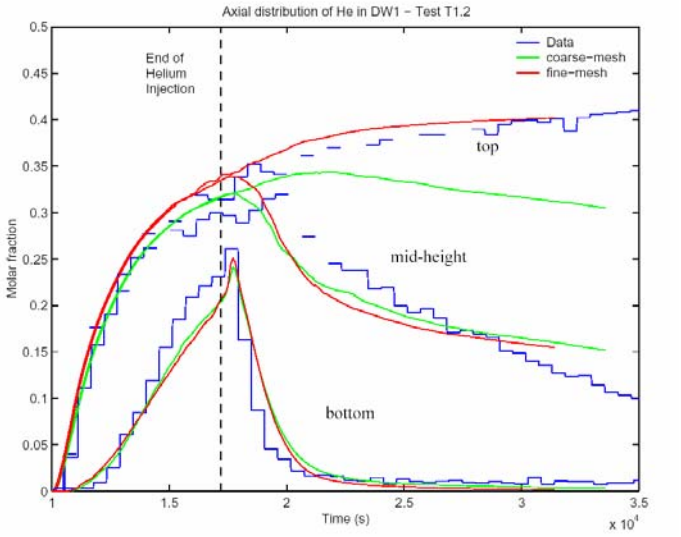

Figure 13: PANDA Test T1.2: Comparison between Calculated and Experimental Helium Molar Concentrations in DW1 at three Elevations

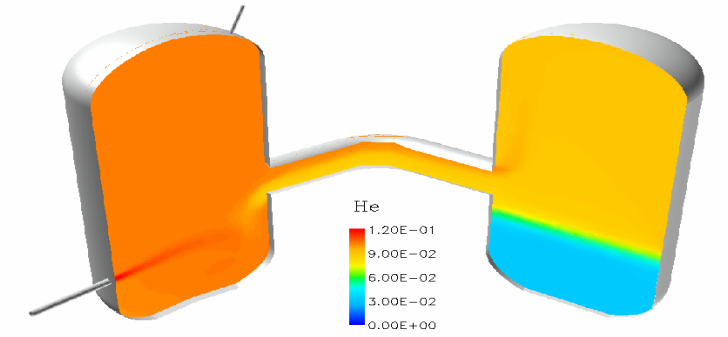

Figure 14: Helium Mass Fraction Distribution in DW1 (right) and DW2 (left), Calculated with CFX-4 at Transient Time 15,000 s into PANDA Test T1.2

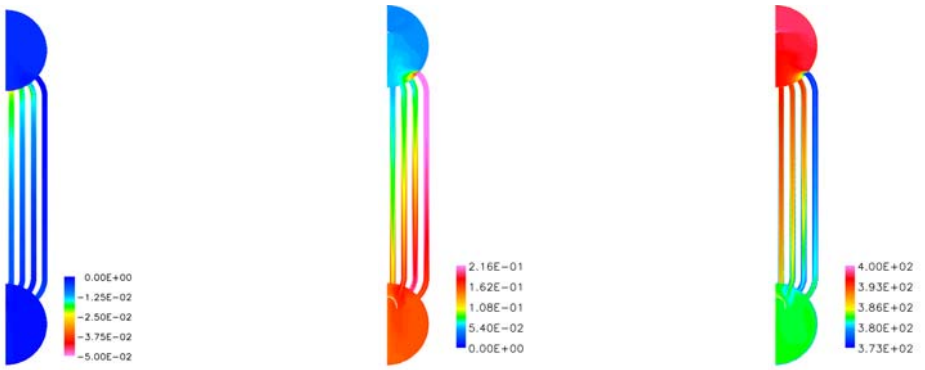

Figure 15: Condensation Flux [kg/m2/s] (Left), Helium Mass Fraction (Centre), Gas Temperature [K] (Right) in the Tubes, CFX-Results Case 2B. PANDA Test T1.2

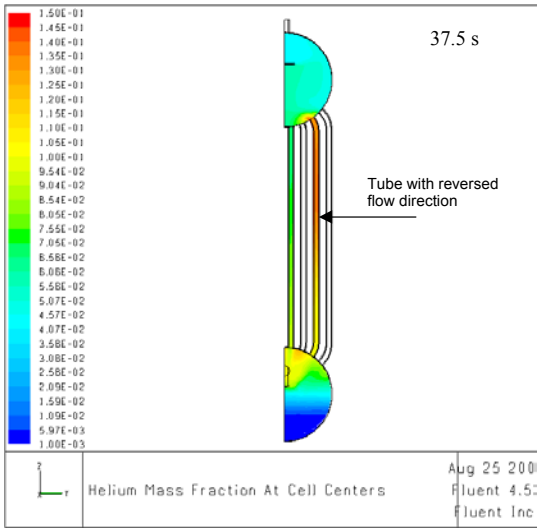

Figure 16: Helium Distribution in a Cross Section through the PCC, Calculated by FLUENT for PANDA Test T1.2

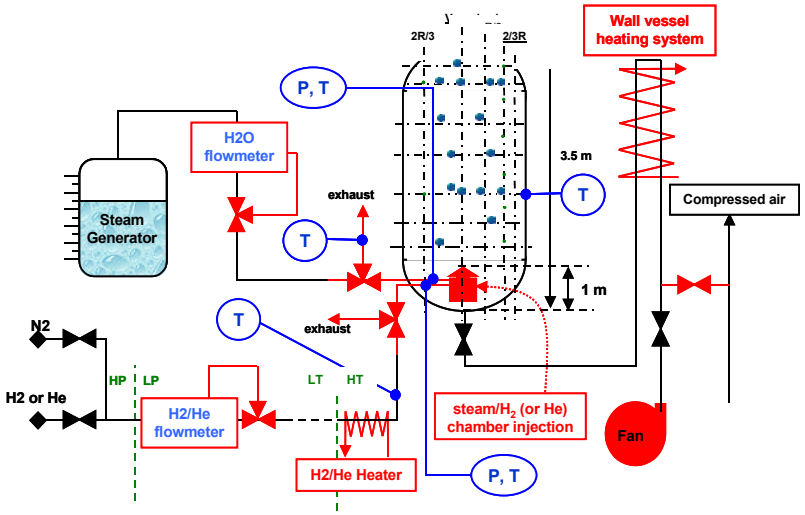

Figure 17: Schematic of the KALI Configuration for TEMPEST Tests

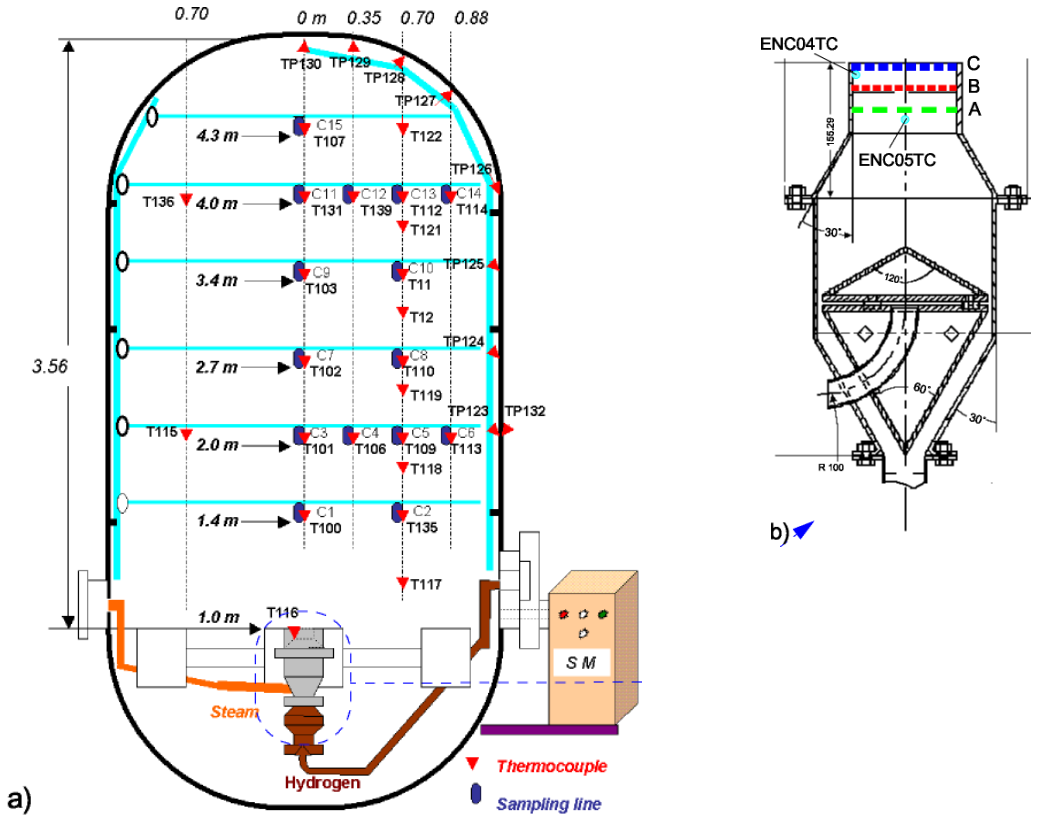

Figure 18: Sensor Locations inside KALI Vessel a) and Mixing Chamber b)

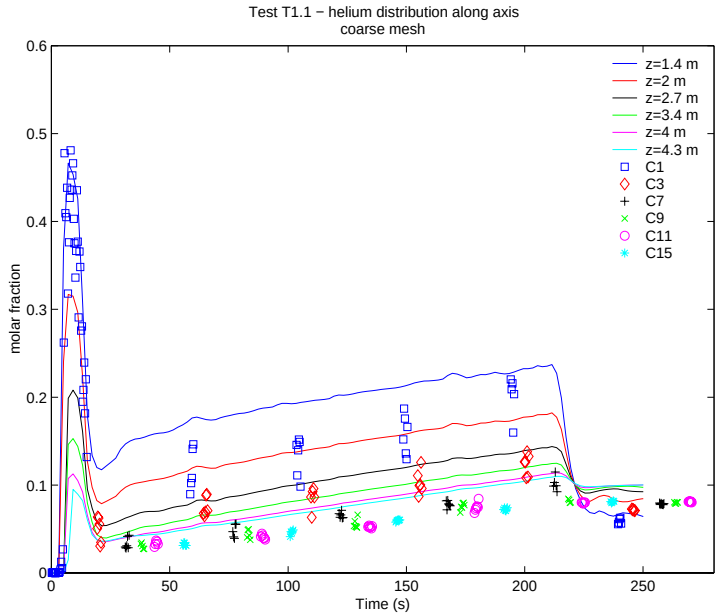

Figure 19: KALI Test T1.1: Comparison between Calculated (GOTHIC) and Experimental Vertical Distribution of Helium along the Axis, Calculated with Coarse Mesh

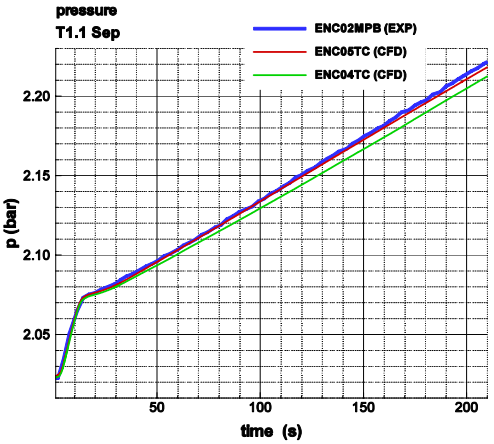

Figure 20:Computed (CFX4) and Measured Pressure for KALI Test T1.1 Sep

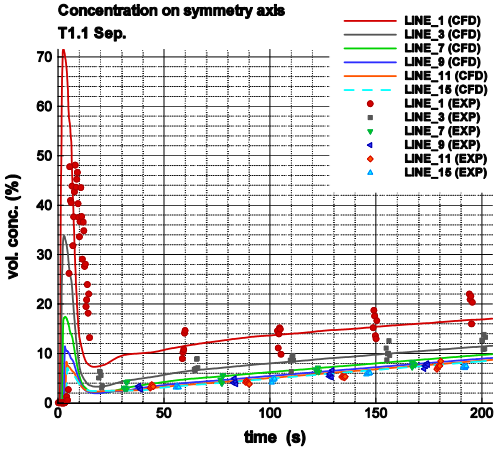

Figure 21: Computed (CFX-4) and Measured Concentrations, KALI Test T1.1 Sep

Figure 22: Temperature, Helium and Velocity Distribution, Simulated with CFX-5, Close to the End of Helium Injection for KALI Test T1.1 (15/10)

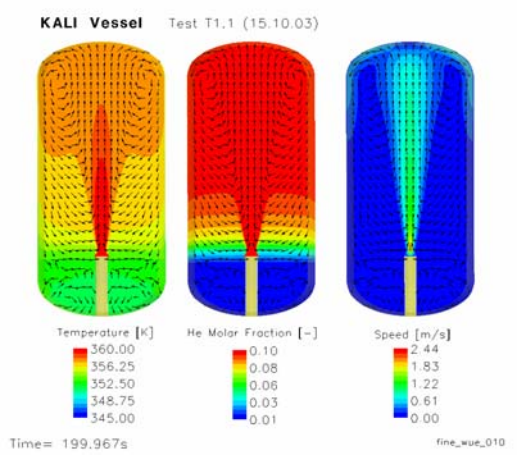

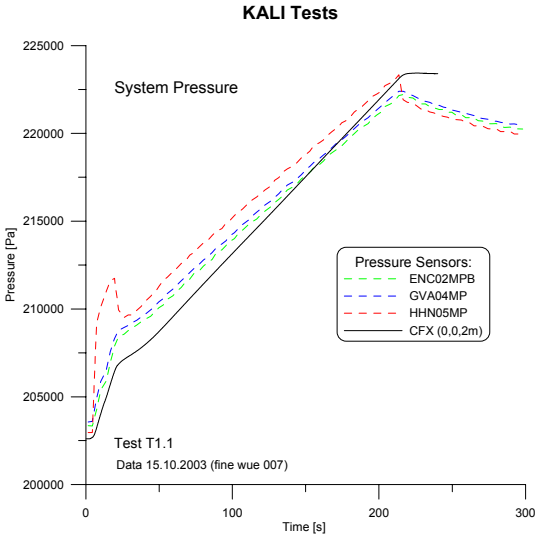

Figure 23: Pressure History for the CFX-5 Simulation of KALI Test T1.1

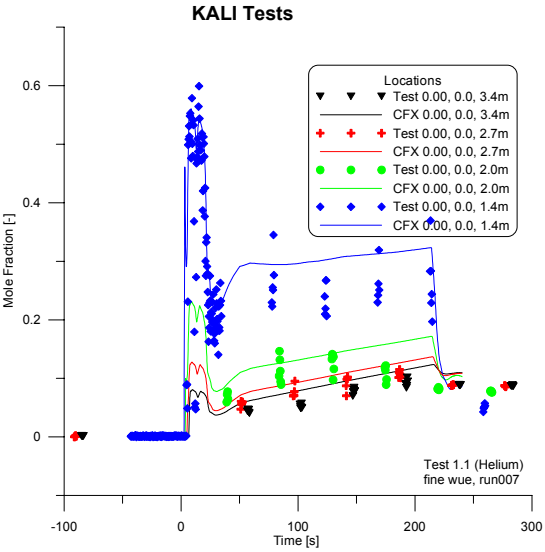

Figure 24: Helium Concentration Simulated with CFX-5 (KALI Test T1.1)

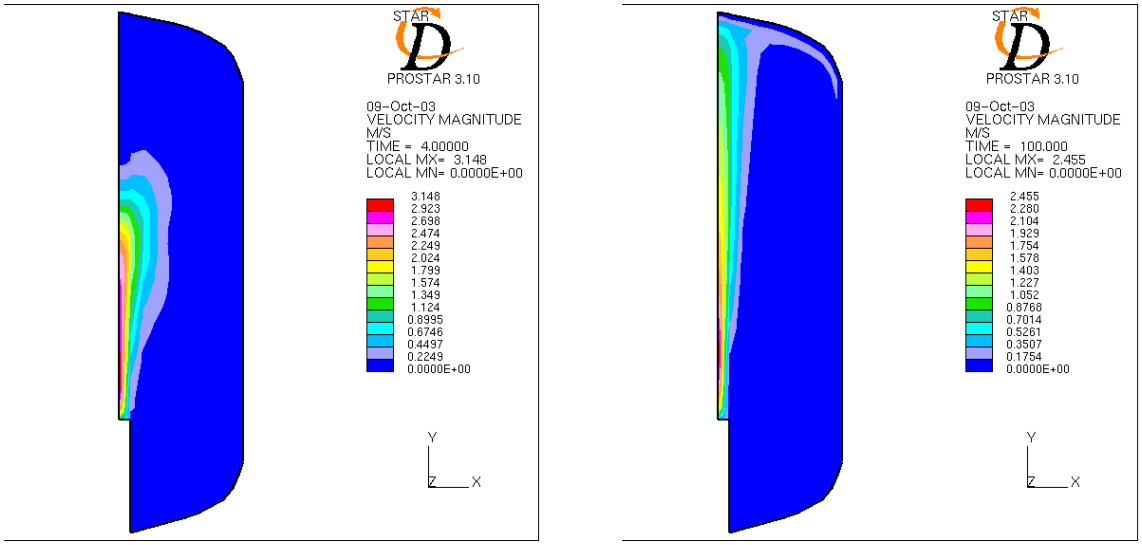

Figure 25: Velocity Fields Calculated with STAR-CD for KALI Test T1.1 at 4 sec (left) and at 100 sec (right)

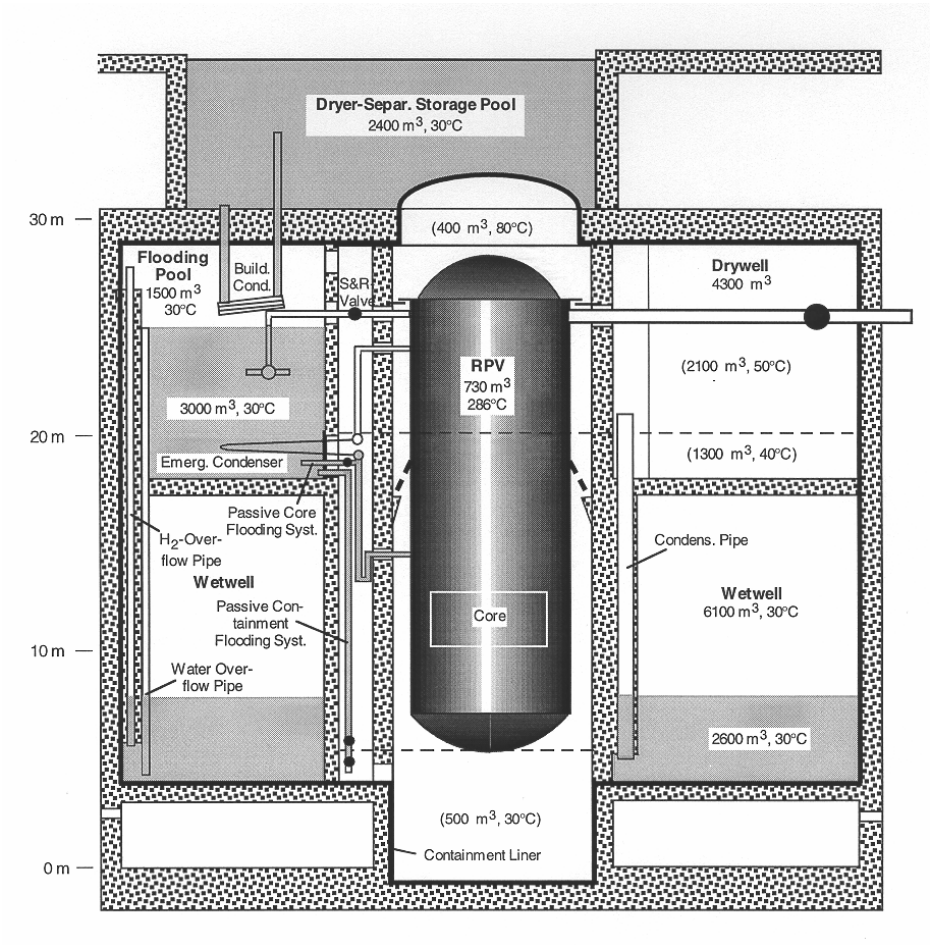

Figure 26: SWR1000 Containment including Passive Safety Systems

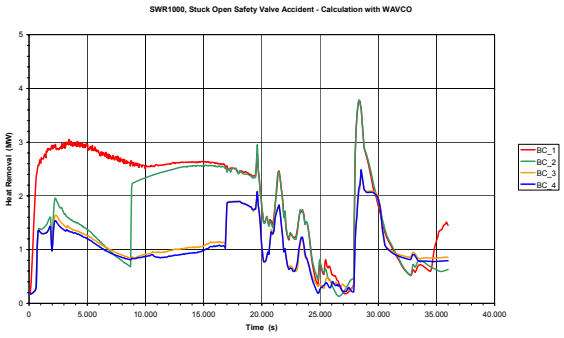

Figure 27: Heat Removal by Building Condensers (WAVCO Prediction)

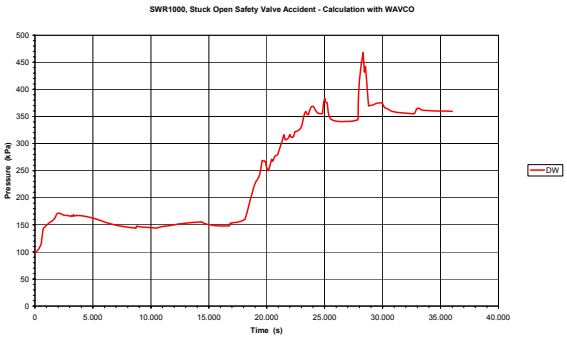

Figure 28: Gas Pressure in Drywell (WAVCO Prediction)

100% Metal-Water reaction (active cladding only)

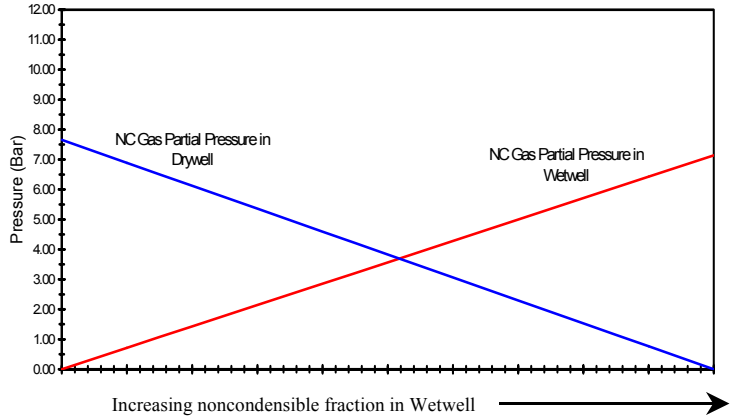

Figure 29: ESBWR Containment Pressure as a Function of Non-Condensable Fraction in the Wetwell for 100 % Melt-Water Reaction

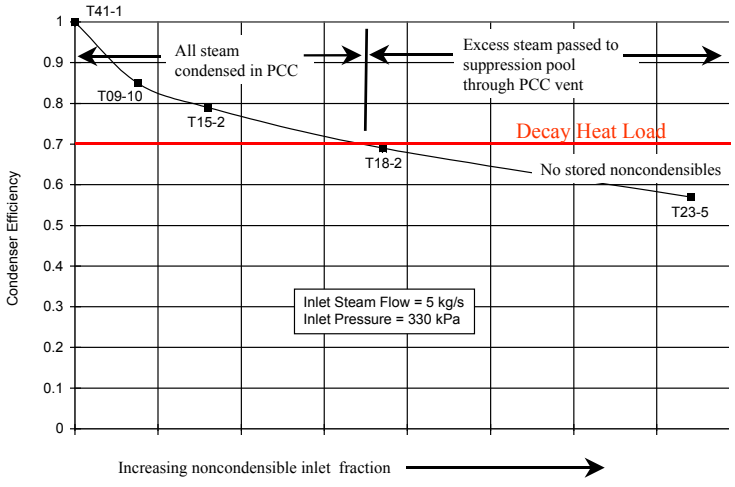

Figure 30: PCC Efficiency as a Function of Non-Condensable Inlet Fraction